Tampere University

Nikita Tafintsev

AERIAL ACCESS AND BACKHAUL IN MMWAVE SYSTEMS

Faculty of Information Technology and Communication Sciences
Master of Science Thesis
October 2019

ABSTRACT

Nikita Tafintsev: Aerial Access and Backhaul in mmWave Systems
Master of Science Thesis
Tampere University
Communication Systems and Networks
Supervisors: Assistant Professor Sergey Andreev and Professor Mikko Valkama
Examiners: Assistant Professor Sergey Andreev and Professor Mikko Valkama
October 2019

The use of unmanned aerial vehicle (UAV)-based communication in millimeter-wave (mmWave) frequencies to provide on-demand radio access is a promising approach to improve capacity and coverage in beyond-5G (B5G) systems. There are several design aspects to be addressed when optimizing for the deployment of such UAV base stations. As traffic demand of mobile users varies across time and space, dynamic algorithms that correspondingly adjust UAV locations are essential to maximize performance. In addition to careful tracking of spatio-temporal user/traffic activity, such optimization needs to account for realistic backhaul constraints. In this work, we first review the latest 3GPP activities behind integrated access and backhaul system design, support for UAV base stations, and mmWave radio relaying functionality. We then compare static and mobile UAV-based communication options under practical assumptions on the mmWave system layout, mobility and clusterization of users, antenna array geometry, and dynamic backhauling. We demonstrate that leveraging the UAV mobility to serve mobile users may improve the overall system performance even in the presence of backhaul capacity limitations. We characterize these gains for the important system parameters and compare our results with those for the static grid deployments.

Keywords: 5G, B5G, UAV, drone, mmWave, aerial, access, backhaul, NR, IAB, PSO, 3GPP

PREFACE

The research conducted in this work was completed in collaboration with Intel Corporation (Santa Clara, California, USA). This work was supported by project 5G-FORCE [1]. I hope that the results obtained in this work will help the research community to continue the integration of aerial wireless networks and will support standardization process in the future.

I would like to thank all my friends and colleagues from Tampere University for their help and contribution to the work. First of all, I would like to thank Assistant Professor Sergey Andreev and Professor Yevgeni Koucheryavy for the opportunity to study and work in Finland. Without their help and guidance, I would have never got such a unique experience. Likewise, I want to thank Professor Mikko Valkama for his support and help. I also wish to thank Dr. Mikhail Gerasimenko for guiding me during my work and study process. This work would not have been completed without his help. Besides, I am very grateful to Dr. Dmitri Moltchanov, Dr. Aleksandr Ometov, and Margarita Gapeyenko for the invaluable suggestions and collaboration in this work.

Finally, I must pay tribute to my friends and family for their patience and understanding in this crucial step of my life.

Tampere, Finland, 23rd October 2019

Nikita Tafintsev

CONTENTS

LIST OF FIGURES

LIST OF TABLES

LIST OF SYMBOLS AND ABBREVIATIONS

3GPP	The 3rd Generation Partnership Project
4G	4th Generation
5G	5th Generation
ALO	Airborne LTE Operations
AP	Access Point
B5G	Beyond 5G
BS	Base Station
CAPEX	Capital expenditures. Funds used by a company to acquire and maintain physical assets such as technology or equipment
CDF	Cumulative Distribution Function. Function, that characterize the probability of X to be lower or equal x, where X is a random variable with given probability distribution
COW	Cell on Wings
CP	Control Plane
DL	Downlink. Data transmission from BS to UEs
E-UTRA	Evolved Universal Mobile Telecommunications System Terrestrial Radio Access
EPC	Evolved Packet Core. LTE core network
FANET	Flying Ad hoc Network
gNB	gNode B (supporting NR and connectivity to NGC)
IAB	Integrated Access and Backhaul
IoD	Internet of Drones
LOS	Line-Of-Sight
LTE	Long Term Evolution. Wireless cellular standard of 4th generation
MAC	The Media Access Control. It is one of the two sublayers that make the Data Link Layer of the OSI model
MIMO	Multiple-Input and Multiple-Output
mmWave	Millimeter-wave. Millimeter-wave is the band of spectrum between 30 GHz and 300 GHz
NGC	Next Generation Core Network

NLOS	Non-Line-Of-Sight
NOMA	Non-Orthogonal Multiple Access
NR	New Radio
NSA	Non-Stand-Alone
OPEX	Operating expenses. An operating expense is an expense a business incurs through its normal business operations
PHY	Physical layer which refers to the implementation of physical layer functions
PSO	Particle Swarm Optimization
QoE	Quality of Experience
RAN	Radio Access Network. Element of a cellular network, main purpose of it is to provide connection to users
RPGM	Reference Point Group Mobility
SA	Stand-Alone
SLS	System-Level Simulator. Simulator, which emulates the network environment
SNR	Signal-to-Noise Ratio
TR	Technical Report
TS	Technical Specification
UAV	Unmanned Aerial Vehicle
UE	User Equipment. Mobile user device used for communication aims
UL	Uplink. Data transmission from UEs to BS
UP	User Plane
VLOS	Visual-Line-Of-Sight

1 INTRODUCTION

The unmanned aerial vehicles (UAVs), commonly known as drones, with their unconstrained three-dimensional (3D) mobility and autonomous flight capabilities, are becoming popular across various applications. Attractive UAV applications for mobile operators include, for example, logistics, emergency services, inspection, wireless connection in disaster-affected regions, and network densification during temporary mass events.

1.1 Commercial Applications of UAVs

Nowadays, commercial UAV applications promise various opportunities and benefits for consumers. In agriculture, for example, UAVs may be used for inspections by observing crop health as well as in logistics as crop spraying tool. Also, many businesses need to inspect properties that are remote and difficult to reach or unavailable because of safety hazards. Therefore, one of the first prosperous commercial applications of UAV technologies has been the inspections of premises. In this case, visual-line-of-sight (VLOS) control is enough and the UAVs batteries can quickly be replaced as needed. Without UAVs, an inspection of these buildings has to be performed manually, which can be costly as it requires experienced workers, professional means and equipment. In contrast, employing UAVs reduces the cost, time and risk to human lives in the case of dangerous areas. The UAVs generally carry a video camera (Fig. 1.1) and possibly other sensors. With the current solutions, the data collected by the UAV is either streamed to a ground control device or stored in the UAV for later retrieval.

The leveraging of UAVs has received significant attention from the businesses and research communities. Today, businesses use UAVs to handle services that need to be performed accurately and with caution. One of the developing areas of UAV applications is transport and logistic. This use case utilizes UAV capability to change its location speedily and easily between two points without being interrupted by restrictions on the ground. Exceptions can be, for example, no-fly zones, such as airports, prisons, and military departments. The UAV can carry a load to the destination as a delivery tool. In this context, the commercial use of UAVs in the delivery industry improves efficiency, lowers costs, and enhances the customer's experience with potentially life-saving benefits in a variety of scenarios. UAVs effectively solve the expensive last-mile problem by sending supplies across the cities or to remote areas.

The utilization of UAVs provides an option for on-demand and same-day delivery as well as the ability to avoid limitations of traditional logistics, such as roadway delays. Over recent years, numerous companies analyzed the use of UAVs. For instance, Swiss Post safely performed over 3000 deliveries in Switzerland for medical services [2]. Also, UPS by cooperating with an emergency company tested UAVs for on-demand emergency deliveries. Moreover, they continued these trials and established a full medical-sample delivery system in North Carolina, USA [3]. One of the most distinguished projects of applying UAVs is Google's project "Wing". It involves UAVs that can carry larger delivery objects. The project "Wing" has become the first UAV company in the USA to receive governmental permission for goods delivery [4]. Nowadays, UAV regulatory documents do not allow flights over people and some city areas, thus restricting operations. Nevertheless, the rules are becoming less severe for businesses employing UAVs.

The next promising use case is surveillance. Surveillance UAVs are used by many government organizations for detecting criminals, also they are used by environment agencies for the management of natural events and threats. They can detect and provide early warning of fires, floods, traffic collisions, oil spills, and other incidents. Besides, UAVs may be helpful in case of natural disasters, such as storms, heavy snow, floods, and earthquakes. Such emergencies might cut off the communication infrastructure, leaving the affected area isolated. In these circumstances, UAVs can be used to collect real-time information about the scale of the disaster. Also, having the swift and correct information, it helps to effectively distribute aid suppliers to the most in need sites.

Figure 1.1. *Unmanned aerial vehicle (borrowed from [5]).*

1.2 UAV-Assisted Wireless Networks

The telecom sector is among those benefiting from active UAV utilization [6, 7]. UAVs acting as base station (BS) carriers, named in this work UAV-BSs, have recently gained increased interest from the academic and industrial communities [8, 9]. This is in part to meet the stringent performance requirements related to ubiquitous coverage, for example, during short-lived and spontaneous events in order to strategically densify the network [10, 11, 12]. Here, the use of conventional BSs may lead to sub-optimal radio resource utilization. Hence, an alternative solution to serve some of the users by the UAV-BSs may boost the capacity and improve resource efficiency [13]. Particular interest is dedicated to the UAV-BSs equipped with fifth-generation (5G) New Radio (NR) capabilities that are able to support a large number of users while satisfying the desired data rate and latency requirements [14]. The airborne deployment has been considered as an alternative to ensure universal cellular access from the flying cell toward terrestrial users in required areas during temporal and large public events.

Following the trend and practical demands, prominent high-tech industrial communities have already initiated several programs towards the leveraging of UAVs. For example, Nokia Bell Labs flying-cell allows providing additional capacity and coverage meaning that the flying small cell may be deployed universally (Fig. 1.2). Next, AT&T developed a flying Cell on Wings (COW), which can provide additional Internet coverage. Besides, Verizon's project called Airborne LTE Operations (ALO) started to facilitate a wireless connection to remote mobile users. Also, Facebook's project using solar-powered UAVs can provide

Figure 1.2. *UAV acting as BS carrier (borrowed from [15]).*

access to the Internet to hard available areas. Another domain of interest for the usage of UAVs is mobile relays. Mobile relays are capable to provide wireless connectivity to users without their direct transmission links to the BS. Links may be blocked by any physical obstacles like buildings or trees. In this type of scenario, UAV can transfer data traffic from the source to the destination aiming to achieve higher system throughput.

With this in mind, different features of UAVs are required for the setup of a multi-tier framework for prospective UAV deployments. These features are mostly aerodynamics characteristics, which include flying altitude, energy savings, maximum allowed payload, maximum flying time, etc. Taking into account these constraints, it was further proposed that the coordination and collaboration of multiple UAVs may constitute flying ad hoc networks (FANETs), Internet of Drones (IoD), and even swarm of UAVs similar to birds (Fig. 1.3). It is envisioned that the usage of a swarm of UAVs potentially will bring a lot of benefits to the 5G cellular network, for example, the better quality of experience (QoE) and higher spectral efficiency.

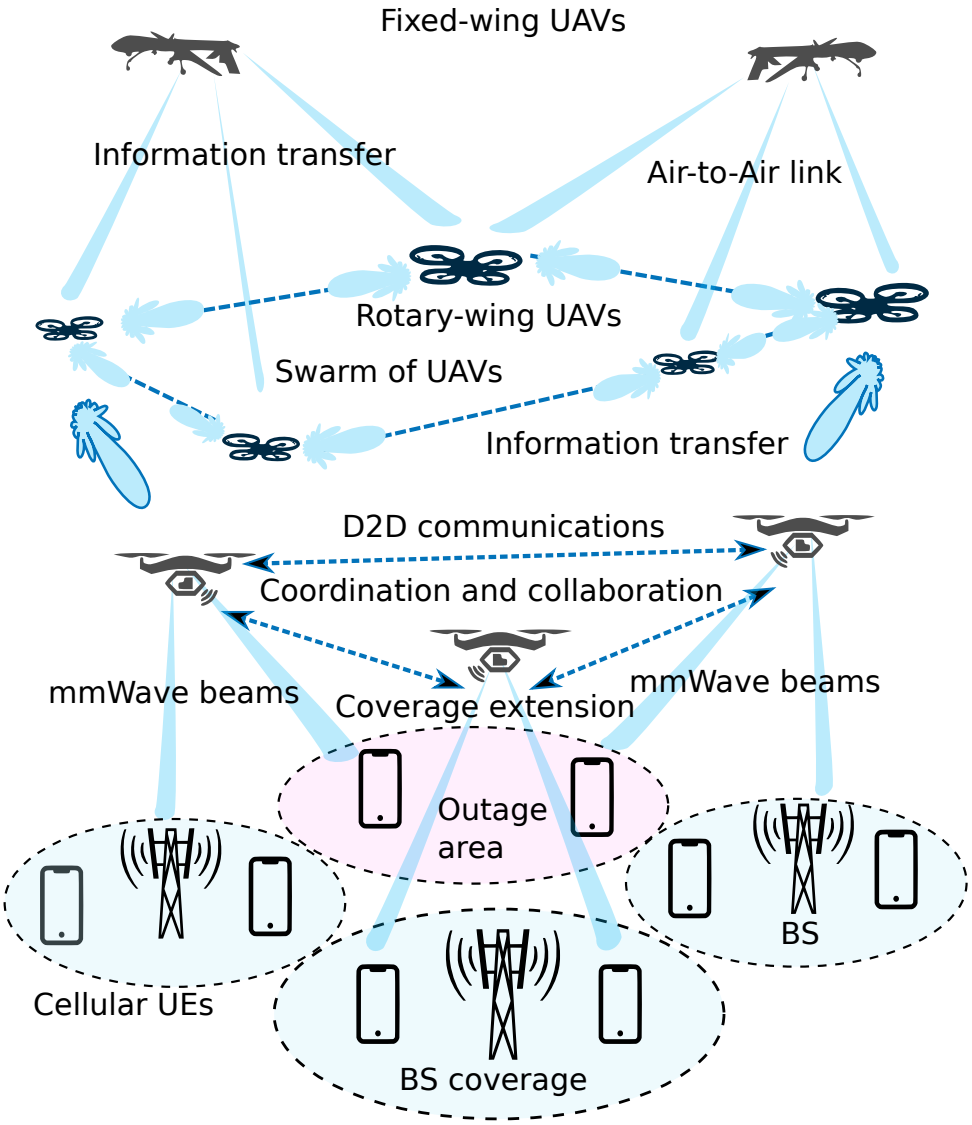

Figure 1.3. *UAVs in wireless networks.*

It can be observed that the various use cases of UAVs have significantly affected wireless networking. The networking strategy to be used in a swarm of UAVs has gained increased interest from both the research community and industry. In addition, there are other typical use cases of UAV-assisted wireless networks. It is worth noticing the following applications: wireless sensor networks [16], UAV mesh networks [17], wireless powered networks [18], caching UAV-assisted wireless networks [19], mobile edge computing [20], device-to-device (D2D) communications [21], etc.

1.3 Scope of the Thesis

To fully benefit from the utilization of UAV-BS and optimize the system-level performance, careful placement of the UAV-BSs is essential. There is a number of factors that affect the positioning of the UAV-BSs. One of these is backhaul connectivity between the UAV-BSs and the core network, which may impact the overall system performance. To yield realistic conclusions, the modeled scenario must be practical, where users can move, cluster into groups, etc. While various algorithms for optimized UAV-BS deployment have been proposed in recent literature [22, 23], there is a lack of comprehensive study considering all of the important factors under practical modeling assumptions.

There is an inherent trade-off between the number of UAV-BSs and service costs. On the one hand, the network operator should provide high data rate coverage to users. On the other hand, due to the partial loading of the network, an ultra-dense network of UAV-BSs may not be suitable in terms of capital expenditures (CAPEX) and operating expenses (OPEX). Another reason to limit the number of UAVs is that an average user cannot afford expensive service.

In this work, we study a challenging problem: deploying a limited number of UAVs in a relatively wide area. The goal of this work is to evaluate the performance of UAV-aided radio systems enabled by integrated access and backhaul (IAB) capabilities with the aid of system-level simulations [24]. The IAB technology is employed in terms of millimeter-wave (mmWave) spectrum utilization for both UAV-BS to user equipment (UE) access and UAV-BS to ground cell backhaul connections. Our evaluation emphasizes realistic deployments with moving and clustered users, practical antenna arrays at both the UAV-BS and the UE, as well as terrestrial infrastructure based on mmWave access points (APs).

We characterize the impact of UAV-BS backhaul dynamics on the system performance by comparing it with the case of ideal (always sufficient) backhauling. The benefit of dynamic adjustment of UAV-BS locations is shown via contrasting two alternative UAV-BS positioning options: grid deployment and dynamic IAB optimization. On top of this, we provide an updated review of the 3rd Generation Partnership Project (3GPP) activities for UAVs, IAB design, and NR-based relaying.

1.4 Structure of the Thesis

The rest of this text is organized as follows. In Section 2, we review the current 3GPP activities in supporting UAVs, IAB design, and NR-based relaying. In Section 3, we explain the advantages and challenges of mmWave-based aerial networks. In Section 4, our simulation approach, system model, and metrics of interest are presented. Section 5 provides illustrative numerical results by comparing static and dynamic IAB solutions under realistic deployment considerations. Conclusions are drawn in the last section.

2 TECHNOLOGY BACKGROUND

In this section, we outline the ongoing and planned 3GPP activities instrumental to employing UAVs for IAB in 5G NR systems and beyond. First, we concentrate on UAV support in cellular systems, we overview use cases and challenges of UAV communications. Then, we proceed by introducing feasible IAB architectures and implementation options. Finally, we review the capabilities of underlying NR relays as important technology enablers.

2.1 Mobile Cellular Generations and the Concept of 3GPP Releases

Mobile cellular technology is developing within a globally agreed framework that defines different generations of technology. Specifically for 3GPP standards, this framework is determined in the concept of incremental releases of a standard. Each mobile generation specifies a set of system capabilities and performance metrics. Typically, since radio interfaces and network performance are evolving, the new generation has more advanced capabilities over its predecessors. The current widely deployed generation of mobile technology is the fourth generation (4G) which 3GPP has standardized under the name of Long Term Evolution (LTE). The fifth generation of cellular networks is currently under development.

3GPP standards are regularly updated in the form of 3GPP standard releases. Each release comprises compatible specifications for all the standardized system segments and interfaces. 3GPP releases normally are backward compatible with previous releases, which allow implementations of the previous releases match correctly with the ones of the new releases. Following this principle, 3GPP can improve existing generations, as well as working on new generations of cellular networks. Therefore, a 3GPP release contains specifications for various generations of mobile cellular networks.

In each 3GPP release, new features for the standard are detailed using a three-stage model. In stage 1, the requirements are developed. In stage 2, the technical solution is developed at an architectural scale. In stage 3, the protocols to maintain the solution are determined. The following diagram (Fig. 2.1) demonstrates a high-level view of 3GPP releases related to UAVs.

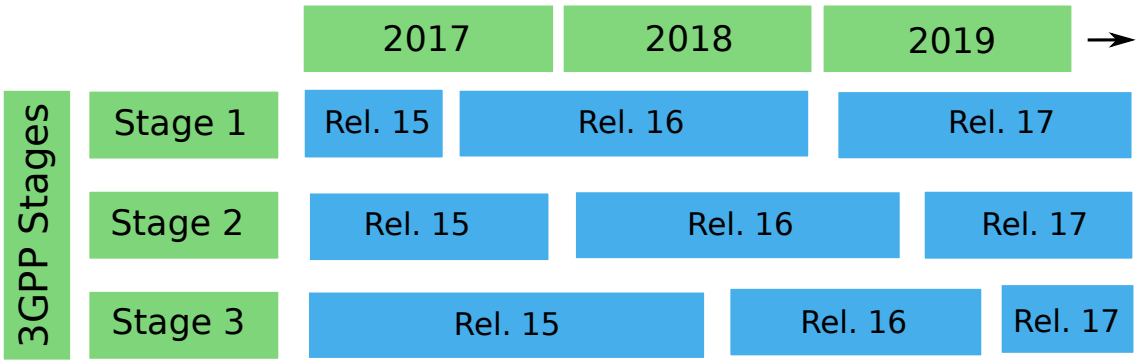

Figure 2.1. *High-level timetable for 3GPP releases and work items related to UAVs.*

2.2 UAV Support

There is a massive interest in the usage of cellular networks to provide support to UAVs. This support may involve leveraging in-flight commands and control systems as well as support for communication to payload applications. Although cellular networks were originally planned for terrestrial users, they are capable of providing strong support to low altitude UAVs. As the number of UAV users grows, the network operators and telecom industry are making an effort to further improve the services provided to UAVs.

Modern cellular networks are designed to comply with common standards that ensure that equipment from different vendors is interoperable. This forms a competitive market for cellular equipment by giving both network operators and customers the option to select the appropriate vendor. All main industrial cellular networks follow the standards developed by the global partnership 3GPP. The standards include the well-established 4G LTE standard and the recently developed 5G standard.

Over the recent years, UAV support and integration into the contemporary wireless systems have received significant industrial interest. Starting from Rel. 15, 3GPP has incorporated the corresponding capabilities into cellular standardization. In this context, the prospective Rel. 16 (see TR 22.829) summarizes the use cases and analyzes the UAV features that may require enhanced support. This includes live video broadcasting applications, command and control communications, and the use of UAV-BSs. The latter is specified in TR 38.811.

In Rel. 15 TR 36.777, 3GPP conducted a study on extended LTE support for aerial vehicles, which facilitates the use of cellular technologies by UAV-UEs. Initiated in 2017, this study summarizes possible cellular system improvements for efficient service of UAV traffic and its effects on the network. Particularly, it evaluates the performance of UAVs in urban and rural micro- and macrocell environments. Extensive simulations supplemented with field measurement data demonstrate that the usage of UAVs leads to increased uplink (UL) and downlink (DL) interference. Further, this work specifies important interference mitigation techniques. Also, TR 36.777 identifies methods to provide additional path information that may be used in making mobility-related decisions.

Further areas that require development include aerial UE detection and identification [25]. This relates to, for example, determining whether the UAV is permitted to fly. The 3GPP Rel. 16 TR 22.825 outlines the requirements for remote identification and tracking of UAVs linked to a cellular subscription. It also discusses the mechanisms for remote identification of UAVs.

Currently, 3GPP continues to explore the ways for cellular systems to further support UAVs. This involves work on improving mobility performance, business, security, and public safety needs for the purposes of identification. To that end, Rel. 16 TR 22.125 identifies the operating requirements for 3GPP systems. In this direction, 3GPP is expected to enhance the support for UAV connectivity and tracking in TR 23.754 and TR 23.755. Clearly, UAVs are capable of accommodating a wide range of use cases for emerging NR technology. One of such important scenarios is IAB (Fig. 2.2).

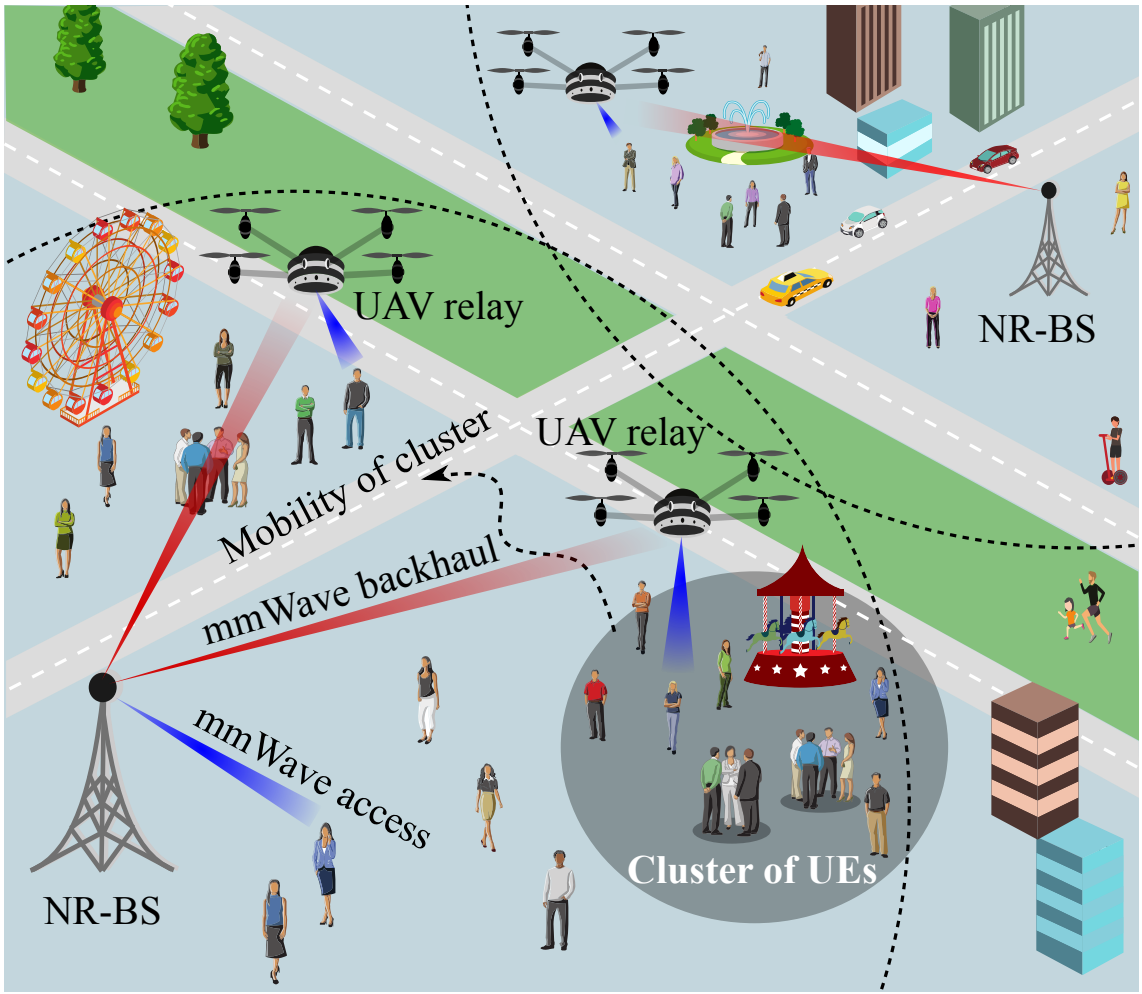

Figure 2.2. *Usage of mmWave-based UAV-BSs.*

2.3 IAB Technology

The standardization of the IAB was initially proposed by AT&T, Qualcomm, and Samsung in the dedicated work item description, RP-171880. The corresponding study item led to the composition of TR 38.874, “NR; Study on Integrated Access and Backhaul”, which summarizes all the activities related to the NR IAB. As depicted in Fig. 2.3, the valid structure of an IAB wireless network consists of several IAB-nodes, which hold wireless backhaul connections and may be served as APs for UEs as well as other IAB-nodes. Besides, the architecture includes an IAB-donor which has fiber connectivity with core network and also may serve UEs and IAB-nodes.

Compared to terrestrial NR deployments, a major limitation of mmWave-based UAV-BSs is their backhaul link. Ground APs typically have a fixed wired backhaul connection and can offer very high data rates to the core network, whereas UAV-BSs should rely solely on wireless backhauling. The concept of utilizing a single radio technology to provide both access and backhaul connectivity has been addressed in 3GPP’s TR 38.874. With the introduction of NR systems, which support highly directional antenna arrays, UAV-BSs equipped with the IAB functions (named here UAV-based IAB) may facilitate on-demand network densification, thus efficiently avoiding interference and reducing capital investments into mobile infrastructure.

Initially, the benefits of IAB for NR were justified in RP-171880. Further, the concept was developed in TR 38.874. Currently, the term IAB is defined by 3GPP in the context of an IAB-node: *“IAB-node is a RAN node that supports wireless access to UEs and wirelessly backhauls the access traffic”* (see TR 38.874). 3GPP does not enforce any particular IAB implementation, which leaves specific details for vendors to decide upon. From the radio network planning perspective, available options include single-hop vs. multi-hop

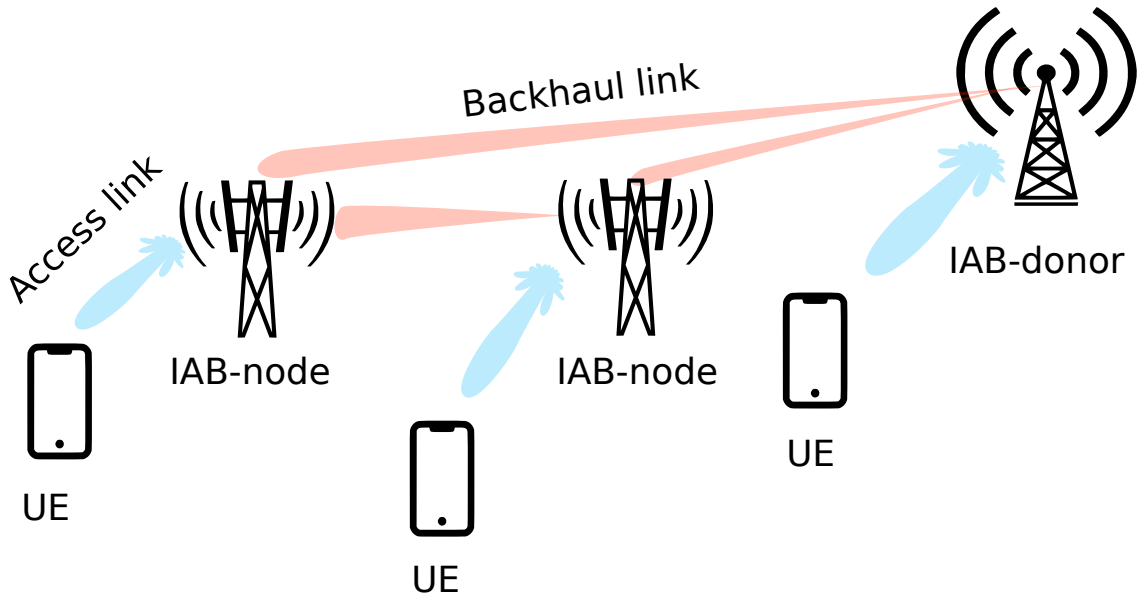

Figure 2.3. *Basic architecture of an IAB network.*

implementations, in-band vs. out-of-band backhauling, various radio technologies in use by the access link, as well as the levels of access and backhaul integration. Therefore, there are plenty of options to choose from, with their advantages and drawbacks.

Although multi-hop backhauling can offer a performance boost for the network coverage known as range extension, it also brings additional overheads in terms of signaling. On top of conventional network management procedures (random access, handover, power control), both multi-hop and single-hop IAB systems need to enable relay-specific functionality, such as backhaul link discovery, management, and re-establishment; backhaul/access resource allocation and coordination; backhaul cross-link interference management, etc. Finally, there is a number of 3GPP-specific protocol-related options considered in TR 38.874, which account for the ways to realize multi-hop forwarding and Evolved Packet Core (EPC) anchoring choices for both the UE and the relay nodes.

The radio technology and its frequency band [26] on the access and backhaul links is another system design choice. For example, if both connections are implemented with the same radio, there is a possibility to utilize joint resource allocation mechanisms, which may reduce the overall system capacity but can also lower the deployment costs. Further, if both access and backhaul links operate over the same frequency band (in-band backhaul), there is a need for additional interference management. According to TR 38.874, the IAB-node should be capable of providing multi-radio access functionality, with at least Rel. 15 NR and legacy LTE options.

Finally, addressing the UAV-specific features, mobility of a relay node should be considered as one of the key benefits of the UAV-based architecture. Some solutions, however, imply static UAV-based relays, in which the access point can be connected to EPC using wired backhaul. In fact, such deployments were already tested by AT&T in emergency situations in which ground network suffered "near-total break-down". In that case, UAV-based relay node is deployed in a way to maximize coverage, that means that mobility of drone can be limited, while power and backhaul links are provided from the ground-based vehicle via the wired connection. However, if UAVs are used in non-emergency situations, mobility of the drone can be used to boost both coverage and capacity performance of the ground-based network.

On top of these architectural choices, the implementation of IAB may differ with respect to the levels of backhaul and access integration. For instance, one can implement separate PHY and MAC realizations for access and backhaul, while sharing certain elements of MAC scheduling in a common module [27]. The IAB is characterized by a range of system design options that have to be further investigated in order to ensure its optimized performance. In addition, NR-based relying is the crucial underlying technology which is currently being ratified by 3GPP. The function of NR relay is the primary technological component for implementing the IAB NR.

2.4 NR Relaying

NR relaying with IAB capabilities has been discussed in TR 38.874 initially planned for Rel. 15 and now continued with the focus on Rel. 16. The role of the relay systems is to connect the UE with the donor BS, which is directly anchored on the core transport network. The gaps in NR coverage due to non-line-of-sight or blockage conditions remain a fundamental limitation for prospective NR deployments. In this context, the benefits of IAB relaying for NR are related to densification of the access network for increased reliability without the need to densify the associated transport network.

Accounting for the natural traffic aggregation at the backhaul links, the backhauling of traffic from the relay to the donor BS is attempted over the NR links. As depicted in Fig. 2.4a and Fig. 2.4b, similarly to the NR BS, the NR relay node may operate in stand-alone (SA) (connected to the 5G core network) or non-stand-alone (NSA) regimes (connected to the 4G EPC) as described in TR 38.912, such that most of the technology for NR access in Rel. 15 (see TS 38.300) is reused for backhaul links.

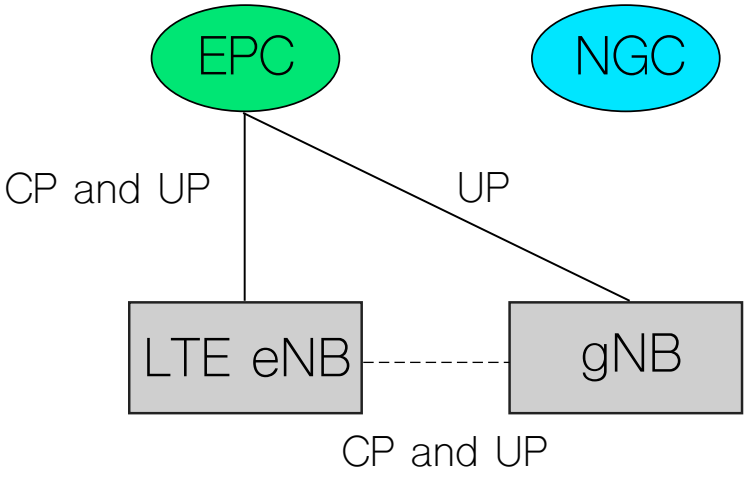

(a) *E-UTRA and NR connected to the EPC*

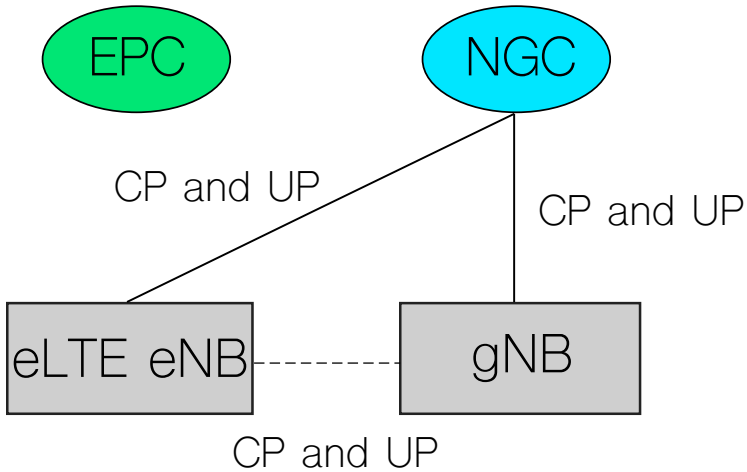

(b) *E-UTRA and NR connected to the NGC*

Figure 2.4. *NR relay node modes.*

The current evaluation results in 3GPP contributions demonstrate considerable benefits from the use of single-hop relaying in the form of decreased outage and increased UE throughput as summarized in TR 38.874. To further exploit the relaying benefits, multi-hop support is presently being discussed by 3GPP (see RP-1806008, RP-1806814, and RP-1806815). The anticipated extra gains from having additional hops, however, pose new challenges related to selecting the best route, optimizing resource allocation, etc. Despite these, flexible multi-hop relaying topology is considered as one of the key components in future B5G systems to connect the UE with the core network. Also, TR 38.874 focuses on IAB with physically fixed relays. Importantly, it does not preclude from optimization for mobile relays in future releases.

The forthcoming Rel. 17 is expected to continue the studies of NR relaying across multiple use cases. One of the considered scenarios discussed in TR 22.866 is the relay support for enhanced energy efficiency and coverage. For example, an industrial factory may rely upon multiple UEs acting as relays to forward traffic from the target UE to its serving BS.

3 ADVANTAGES AND CHALLENGES OF MMWAVE-BASED AERIAL NETWORKS

In this section, we examine mmWave technology key engineering benefits and drawbacks together with possible applications. In particular, we discuss thoroughly the cutting-edge problems, their solutions, and open challenges of 5G mmWave communications for UAV-based wireless networks. Then, we proceed by providing a summary of IAB deployments features.

3.1 Key Advantages of mmWave-based UAV Communications

The current mobile generation (4G LTE) uses the microwave spectrum which lies below 6 GHz. It is clear that this over-utilized domain of the spectrum is insufficient for the upcoming cellular networks to achieve the desired data rates. To overcome limited spectrum availability issues, several enabling techniques have been proposed. These include massive multiple-input and multiple-output (MIMO), non-orthogonal multiple access (NOMA), advanced channel coding and modulation schemes, etc. One of the potential solutions has been expanded to the use of higher frequencies in the radio spectrum. There is still a tremendous amount of available bandwidth at mmWave frequencies, which are dedicated for later usage. In this context, mmWave frequencies, laying between 30 GHz and 300 GHz, play a crucial role in enhancing data throughput in 5G networks.

The use of mmWave bands allows for a dramatic increase in the data rates for mobile users [28, 29]. The excess of unoccupied bandwidth accessible at mmWave frequencies is one of the key benefits of novel 5G networks. The larger available bandwidth implies a remarkably large throughput of 10 Gbit/s, which can be exceeded by introducing, for example, full-duplex enhancements. Likewise, the mmWave bands are attractive for UAV communications as connected UAVs will require enormous data rates, which cannot be delivered by 4G LTE mobile channels. Along with its inherent benefits, the use of mmWave frequencies poses unique challenges to wireless system design.

3.2 Path Loss and Atmospheric Attenuation

The free-space path loss is the loss of signal strength when it propagates through free space between transmitter and receiver. The free-space path loss can be represented in the unit of dB as following:

$$PL = 20\log_{10}(d) + 20\log_{10}(f) + 92.45, \tag{3.1}$$

where d is the distance in km between transmitter and receiver and f is the signal frequency in GHz. The path loss depends on distance and signal frequency. For the microwave signals, the free-space path loss is much lower than for the mmWave signals assuming the same radiation power, antenna gains and distance between the antennas.

Fig. 3.1 shows the free-space path loss for various distances between the source and the destination as a function of signal frequency. As one can observe, the free-space path loss increases with the increasing signal frequency. It is also true that path loss raises for both microwave and mmWave frequencies with the increase of the distance between the transmitter and the receiver. This shows the effect of mmWave frequencies, which limit the propagation distance.

The free-space path loss is merely one sort of signal strength reduction, which happens while propagating through the model vacuum medium. However, in real-life scenarios, mmWave signals propagate in the atmosphere. Therefore, the signal is being affected by

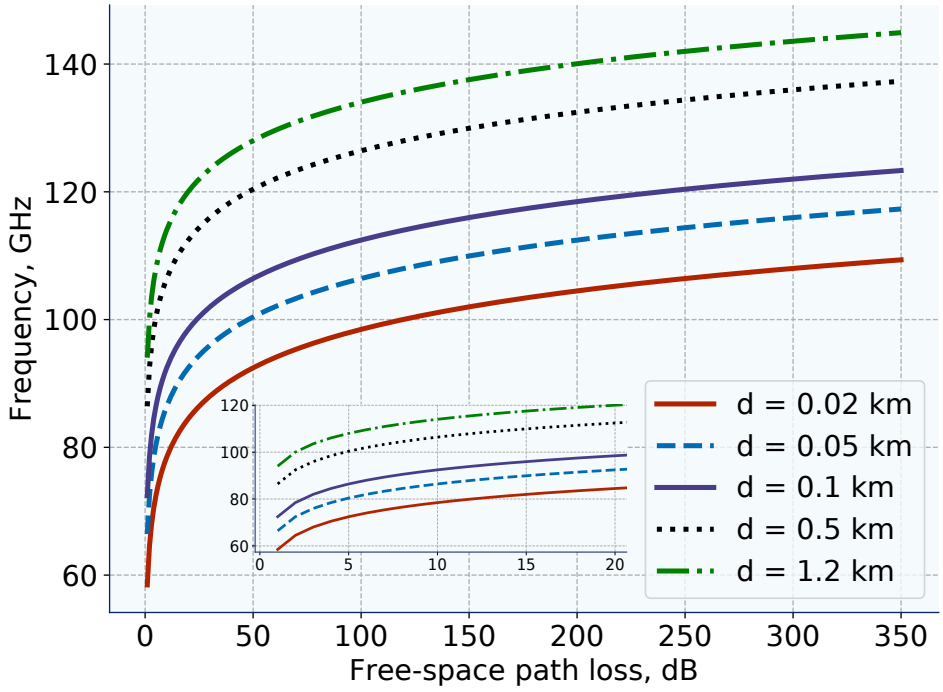

Figure 3.1. *The free-space path loss for different signal frequencies.*

the frequency-related atmospheric attenuation. This effect manifests itself in the form of interaction of atmospheric molecules of oxygen, water, etc. More concretely, the aforementioned particles can absorb a certain part of the signal energy and thus fluctuate with an intensity proportionally to the signal frequency [30]. It is worth noticing that these effects are manageable for frequencies below 10 GHz, whereas for mmWave frequencies, atmospheric attenuation grows dramatically. Moreover, at certain frequencies, due to molecular features, signal attenuation has distinctively large values. Consequently, these effects limit the operational distance of mmWave signals thus affecting the system performance.

Fig. 3.2 demonstrates the explicit attenuation induced by atmospheric oxygen and water molecules. It is easy to see that the signal attenuates significantly at mmWave frequencies, particularly for the water vapor density of 7.5 g/m^3. It can be observed that there are three peaks in the frequencies of roughly 60 GHz, 120 GHz, and 180 GHz, wherein the attenuation approaches the highest values of 14.65 dB/km, 2.0 dB/km, and 27.77 dB/km, respectively. The reason behind these peaks can be explained by the absorption of the molecules at those specific frequencies.

Besides the atmospheric absorption by molecules, weather conditions may radically affect the propagation properties at mmWave frequencies. Since the raindrops are roughly the same order of the size as the wavelengths of mmWave signals, they will add extra attenuation due to scattering and absorption of electromagnetic waves. The effect of rain is demonstrated in Fig. 3.3. It can be seen that the attenuation for mmWave frequencies is much greater than for microwave ones.

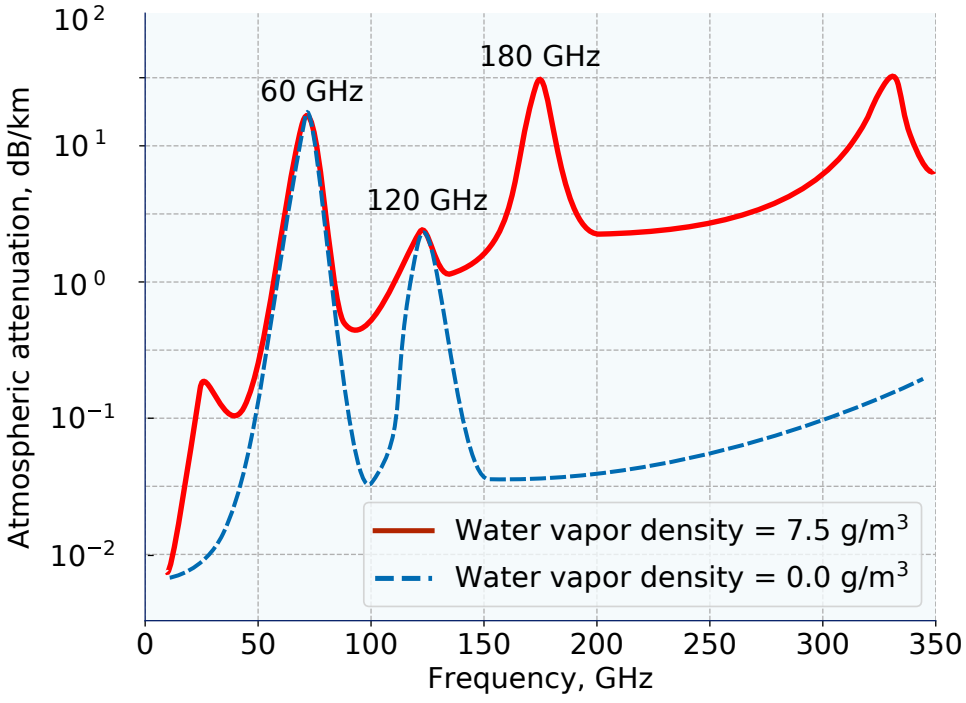

Figure 3.2. *Attenuation induced by atmospheric oxygen and water molecules (reproduced from [31]).*

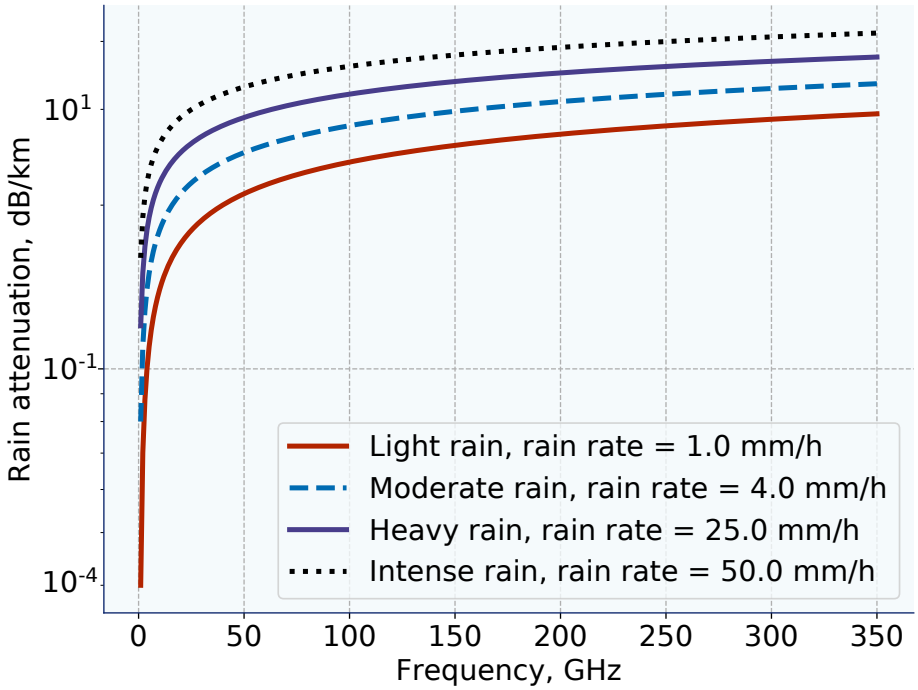

Figure 3.3. *Rain attenuation (reproduced from [31]).*

3.3 Blockage Effect

Another problem of mmWave communications is blockage of line-of-sight (LOS) propagation [32]. Blockage happens when the object or other obstacle blocks transmitted signal thus preventing penetration and creating the non-line-of-sight (NLOS) conditions (Fig. 3.4). It has been pointed out that mmWave LOS and NLOS conditions have notably distinct path loss properties. Penetration into buildings and diffraction provoke higher signal attenuation thus furthering the significance of LOS propagation and reflection.

The path loss of mmWave signals can be caused by various materials and surfaces of the obstacles. Also, the foliage of the trees may decrease the signal strength of the mmWave signals. Based on literature in the field, diverse factors including shape, dimension, and material type of the obstacles have a critical effect on the blockage at mmWave bands. As a result, the high density of blockages of mmWave LOS links and the large blockage duration cause performance degradation of 5G systems. Luckily, reflection and scattering of the signal may help partially alleviate this problem.

To adjust to the spatial variations of the wireless channel, higher gain antennas and directional beams need to be used to compensate for elevated mmWave path loss. Such fast deviations of the channel should be predicted for the peculiar composition of beamforming algorithms. In particular, mmWave transmission requires highly directional transceivers, which significantly lowers radio interference between the nearby communicating nodes thus enabling more flexible positioning and higher network density.

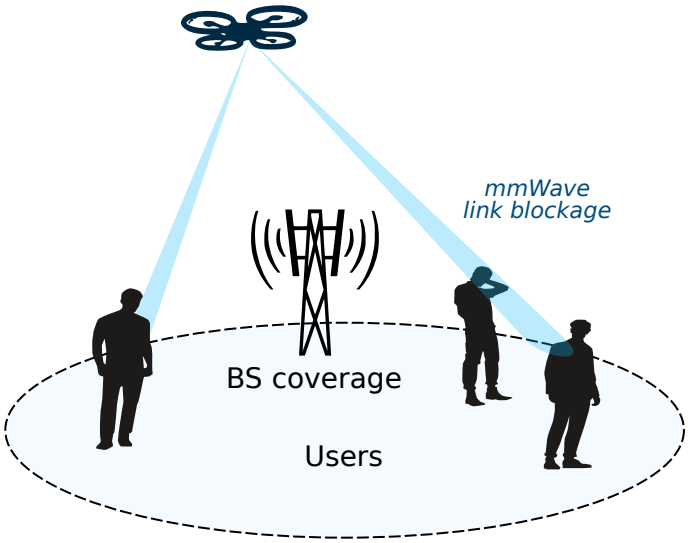

Figure 3.4. *mmWave blockage.*

3.4 Beam Misalignment

One of the crucial components of UAV-based wireless networks with the usage of mmWave technology is the antenna system. The antenna systems act as a means to transmit and receive signals for the UAVs between BS and UEs. In addition, one of the new features of 5G is beamforming.

Beamforming is a radio frequency technology that allows generating directional antenna beams leveraging antenna arrays at the receiver and transmitter [33]. Each of them is able to adjust the direction of signal transmission and determine the best path in order to reach the destination. In particular, beamforming shapes the beams to attain better signal-to-noise ratio (SNR) values. Further, it is feasible to direct the antenna in any direction and avoid undesired signals from an inappropriate path.

Generally, beamforming divides into two types: 2D beamforming, where the beam pattern can be steered only in a certain plane, and 3D beamforming, where a system adjusts the radiation antenna pattern in both horizontal and vertical planes to support more users by adding extra degrees of freedom. The benefits of 3D beamforming include higher network capacity, efficient energy usage, improved coverage, and enhanced spectral efficiency. Moreover, this approach may reduce interference, since additional dimension allows to apply different powers to the beam patterns. Therefore, cell-edge users and users located in the center of the cell acquire separate beams. This method prevents extra power radiation thus decreasing inter-cell interference in the cellular system.

Besides, 3D beamforming may be categorized into static and dynamic. The main difference is in the way in which the antenna's down-tilt is changed. The static 3D beamforming relates to an approach where the antenna's tilt at the transmitter is set to a fixed direction [34]. On the contrary, the dynamic beamforming is a method that changes the antenna tilt without delay according to the precise user positions [35].

One of the feasible techniques to create a beam is to install repeated antenna elements in an array. One of the common methods is to align the antenna along a line. An example of a modeled beam of the linear antenna array is shown in Fig. 3.5. By adding extra dimensions and arranging the elements in an antenna array, one can form a two-dimensional antenna array as shown in Fig. 3.6. In this method, the direction of the radiation beam is changed in both horizontal and vertical planes.

Furthermore, by adding more elements in the antenna array, one can obtain more flexibility in beam sweeping and grow the number of beams of the array. It is envisioned that beam sweeping with beam adaptation for each UE will require a large number of antenna elements. Therefore, one of the difficulties of the beam sweeping is physical restrictions and placement of a large number of antennas at a transmitter and receiver. This challenge can be solved in higher frequencies which are anticipated in 5G mmWave networks.

The beamforming technique allows achieving greater resolution along with the sought directions. Highly directional and narrow beams may be used to compensate atmospheric attenuation and free-space path loss at mmWave frequencies. However, since the shortened beamwidth of mmWave signals and the mobility of users affect the beamforming procedure, it becomes challenging to steer the beams between transmitter and receiver. Therefore, beam misalignment is an inevitable challenge. The misalignment of beams not only decreases the probability of successful transmission and reception but also corrupts the network performance.

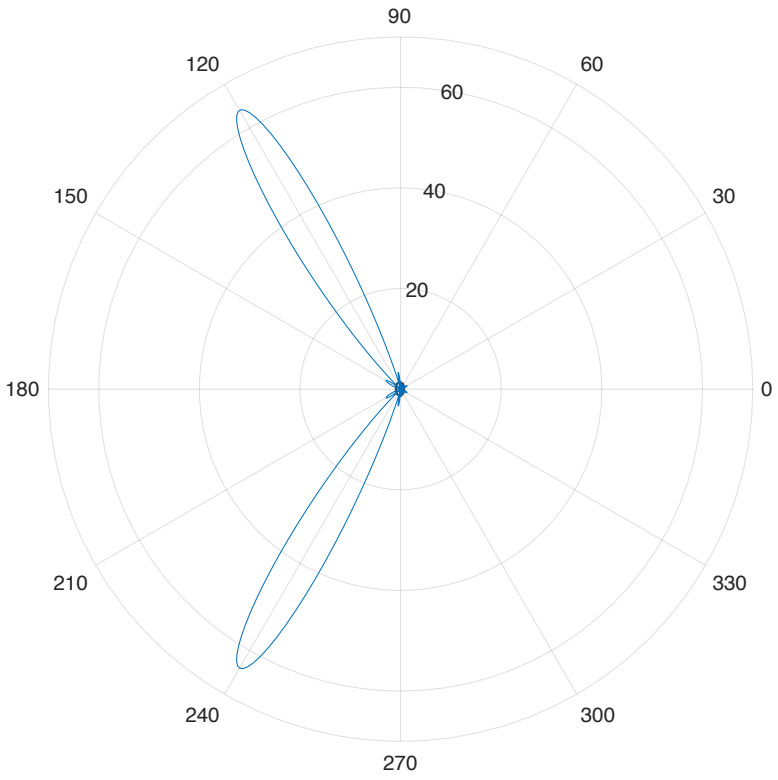

Figure 3.5. *Example of beam modeling.*

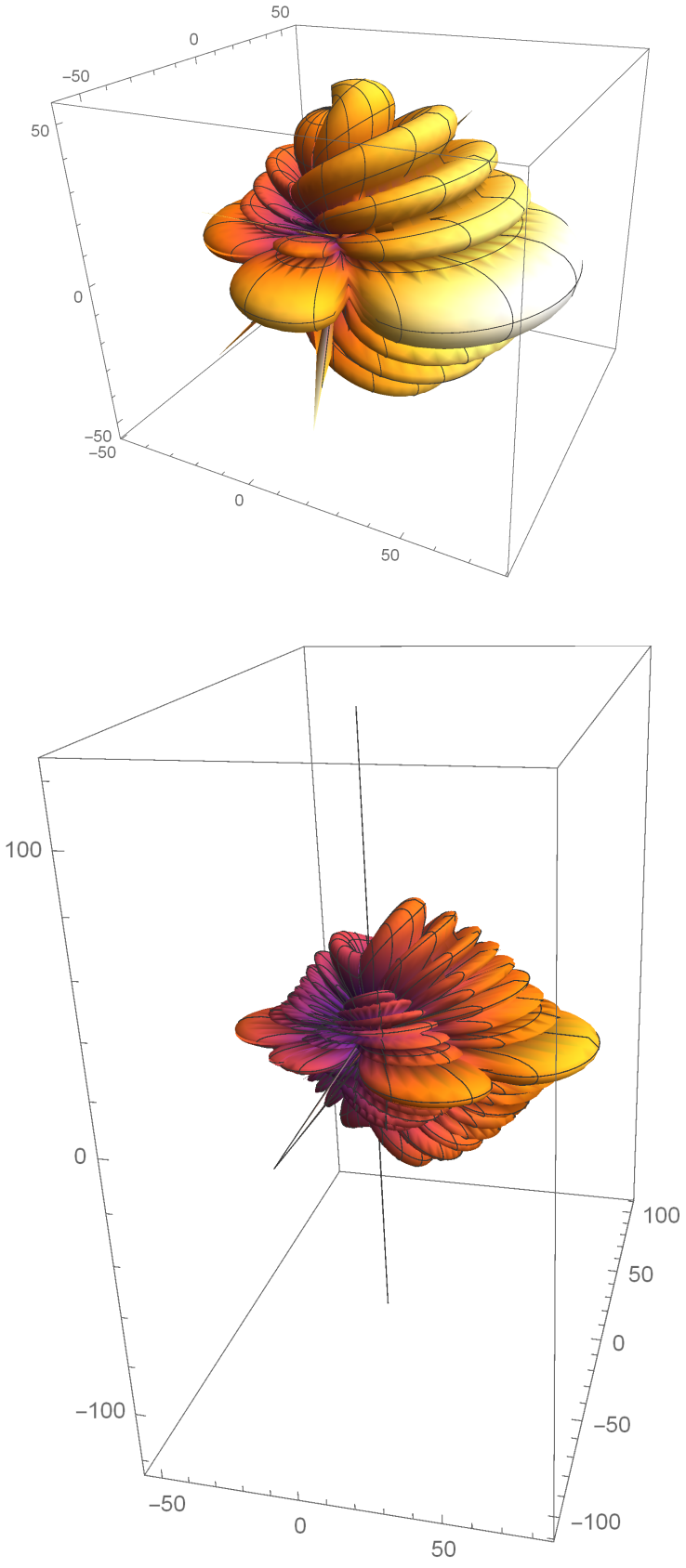

Figure 3.6. *Example of 3D beamforming.*

3.5 Features of IAB Deployments

A broader challenge of radio network optimization has been discussed thoroughly in the past few years. A number of efficient solutions have been proposed for various system settings in heterogeneous networks [36]. However, these do not incorporate the unconstrained mobility of UAV-BSs as well as intricate features of the IAB design, such as the need to account for the NR propagation effects, dynamic UAV-BS associations, and bandwidth partitioning between the AP and the UAV-BS, among other factors. Therefore, the development of more advanced optimization methodologies for the emerging systems that involve UAV-based IAB is of paramount interest for the entire research community.

Recently, the authors in [37] demonstrated that capturing unconstrained 3D deployment of communicating entities inherent for IAB is critical for NR systems operating with directional antennas. However, higher altitudes of UAVs may partially alleviate the problem of dynamic human blockage. At the same time, adding the third dimension is also known to alter the mmWave propagation specifics. Further, it is critical to account for the realistic user placement and mobility patterns. Specifically, IAB systems are expected to be deployed in highly clustered environments with potentially correlated movement patterns, for example, so-called hot-spot areas.

IAB systems providing coverage extension and capacity boost are expected to be deployed on top of the terrestrial NR infrastructure. Serving the moving users, UAVs may continuously adjust their positions and thus the backhaul association point to the anchor NR-BS. Similarly, in realistic deployments, users should also be able to dynamically change their network association point. As a result, a suitable performance optimization algorithm has to be flexible enough to capture these aspects while providing optimized performance at all times.

In previous works [38, 39], the human body blockage analysis of terrestrial mmWave communications was shown. It was demonstrated that adjusting the height of the BS can minimize the blockage probability from the human crowd. However, increased altitudes of the BS lead to the increased path loss due to the larger 3D distance from UE to BS. Particularly, it has been demonstrated that the effect of blockage for 3D deployments of communicating entities is of secondary importance as compared to the exposure probability (the probability that an interfering UAV causes interference at the target UE) produced by the antenna array directivities, especially for modern antenna arrays.

In the past works, the authors assumed static deployments of UEs across a certain area of interest when addressing the positioning of UAV-BSs in 3D space, such that a certain parameter of interest is optimized. However, these studies do not account for potential mobility of the UAV-BSs, which can be efficiently explored to improve network coverage as discussed in [40]. It was also highlighted that the deployment of UEs over the landscape as well as their mobility pattern may not only drastically affect the optimal positioning of the UAV-BSs but also impose further requirements on the choice of the appropriate

optimization methodology. Furthermore, as highlighted in TR 38.874, the backhaul constraints may further impact the optimized UAV-BS locations.

Recent studies address the particularities of the IAB design (see [41]) and advocate for the use of dynamic optimization methodologies. In contrast to conventional optimization techniques that assume static UEs deployments, new adaptive algorithms need to accommodate changes in UE locations by continuously updating the UAV-BS placement within a bounded 3D space to fully benefit from their inherently mobile nature. Most of such solutions are semi-empirical and come from the field of evolutionary computation [42]. Examples of the resultant algorithms include the PSO schemes considered in this work, ant/bee colony optimization, and genetic algorithms. Despite the lack of analytical tractability, they may bring decisive improvements to complex IAB-based system implementations in real deployments, and this is an area where our future research will also focus.

In summary, the latest work indicates that an accurate performance assessment and optimization of the IAB-based NR design requires a number of modeling choices to be specified carefully. Particularly, one needs to (i) account for true 3D layouts for UAV-BS positioning, (ii) rely upon accurate air-to-ground NR propagation models, (iii) employ realistic UE deployment and mobility models, and (iv) incorporate practical B5G deployment considerations.

4 DEPLOYMENT CONSIDERATIONS, MODELING, AND METRICS

This section provides a detailed system model description. First, we concentrate on network layout design and interfaces configuration. Next, we describe a user mobility model used in this work. After that, we characterize an optimization technique based on a metaheuristic approach, which makes no assumptions about the optimization problem and may explore large areas of candidate solutions. In the end, we shortly discuss the simulation approach employing in this work.

4.1 Network Layout

We consider a square area covered by terrestrial NR APs and aerial UAV-BSs offering additional connectivity options for the UEs. We concentrate on studying a relay topology, where APs have two interfaces for the UEs and UAV-BSs (see Fig. 4.1). Likewise, UAV-BSs have two interfaces for the APs and UEs. Further, we assume that based on the signal strength the UE may connect either to the UAV-BS or to the ground AP. The altitude

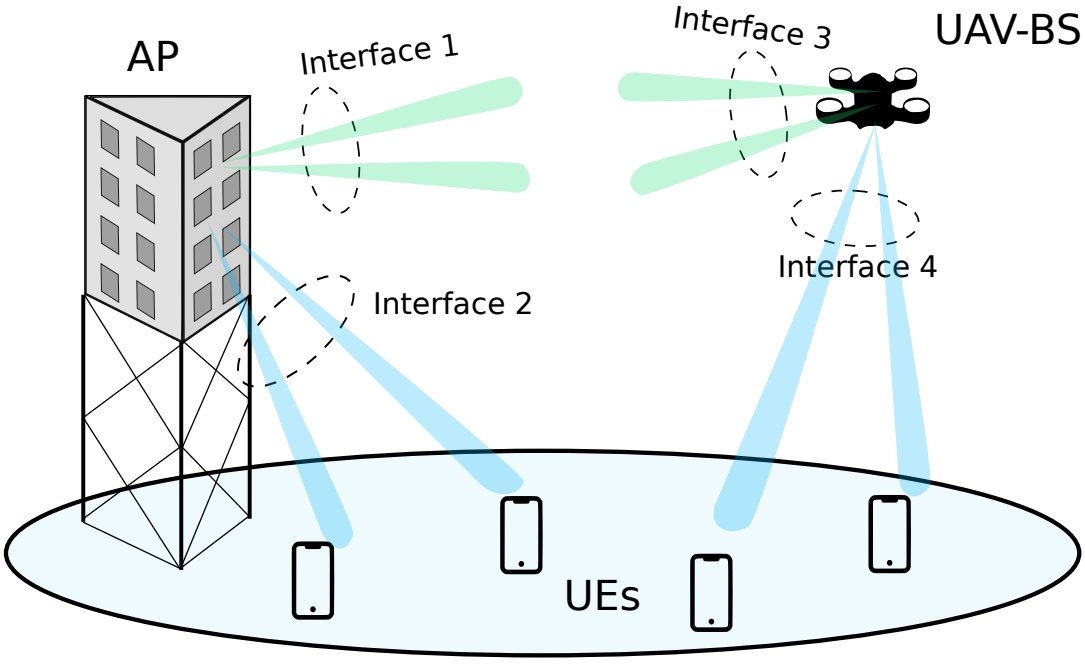

Figure 4.1. *UAV's and AP's interfaces.*

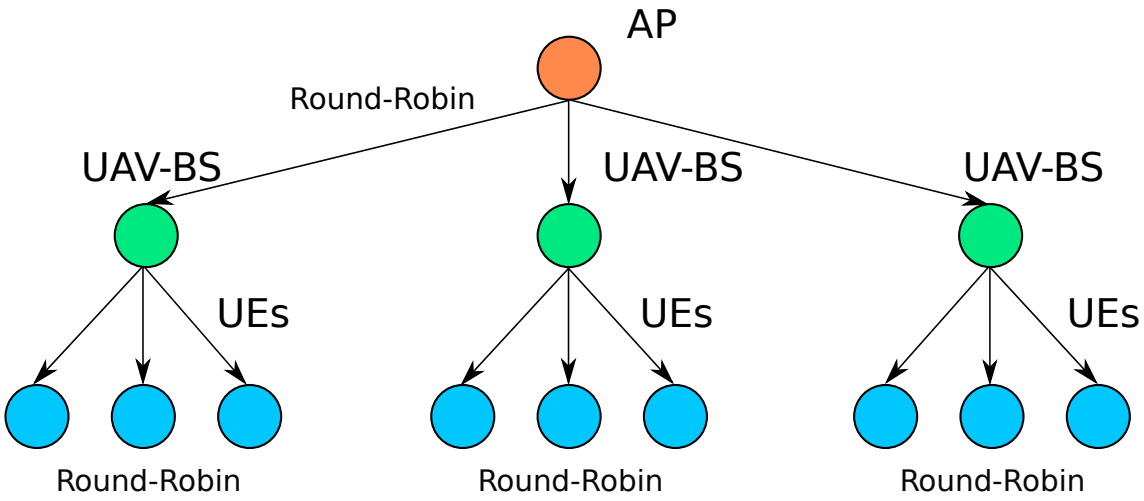

Figure 4.2. *Network layout.*

and the speed of UAV-BSs are fixed, and the latter can only alter their directions in the horizontal plane. We concentrate on the UL direction from the UEs to APs by considering constant traffic from the UEs.

In the addressed scenario, APs act as traffic sinks, since the UL traffic from the UEs to UAV-BSs is further forwarded to the APs (Fig. 4.2). We also require packet buffers on the UAV-BSs and UEs. Packets are queued at the UAV-BSs: if the UAV-BS buffer is full, it drops any arriving packets. UAV-BSs aggregate all of the received packets and send them to an AP currently having the best channel conditions. In this work, we assume separate channels for access and backhaul links (i.e., out-of-band backhauling) as well as dedicated antenna arrays for each interface. In practice, it means that an IAB node is equipped with two separate PHY interfaces, which run independent MAC schedulers, whereas routing, packet queuing, and other procedures are coordinated by the common IAB entity. At the UE to AP and UE to UAV-BS interfaces, we follow α-fairness as a broad class of utility functions that capture different fairness criteria [43].

4.2 User Mobility Models

It is clear that mobility models are application dependent. For modeling, the behavior of users can be specified using simulation models, which consider detailed and realistic mobility scenarios. Various mobility models may be used, as they play a crucial role in simulations of cellular networks. In [44], the authors investigate mobility patterns in wireless networks. They describe various mobility types that represent nodes, whose movements are independent of each other as well as introduce several group mobility models. The authors claim that the most general out of the characterized group mobility models is the Reference Point Group Mobility (RPGM) model. Specifically, at least three models (Column, Nomadic, and Pursue) can be accomplished as particular instances of the RPGM model.

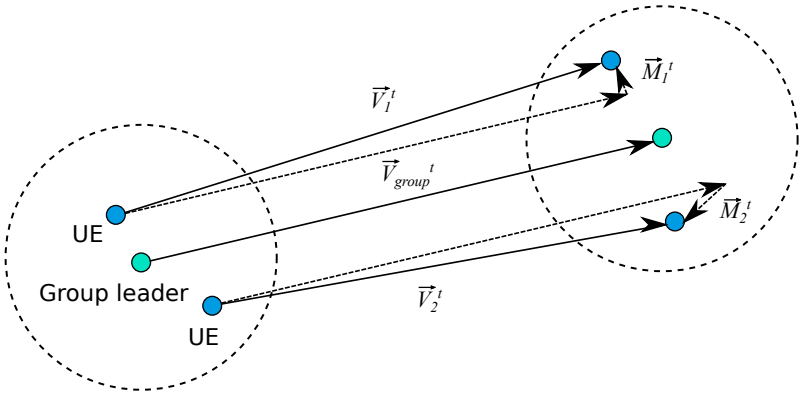

Figure 4.3. *Reference Point Group Mobility model.*

In what follows, we investigate cases where the spatial density of users varies over time. For instance, it may be a mass event, such as a feast or a celebration. To model group user mobility, we employ the RPGM model [45] (see Fig. 4.3), where each group of users has a leader, whose movement determines the mobility direction of the entire group. In the RPGM model, the users are organized in groups according to their actual relationships. Particularly, each group has a leader, the mobility of which determines the whole group's motion, including positions, the direction of movement, speed, and acceleration. The model captures the mobility of clusters by setting a path for each cluster. A path that a cluster will pursue is given by determining a sequence of points along with the path corresponding to given time intervals.

In this mobility model, the movement of a group center at time t can be specified by a movement vector $\vec{V}^t_{group}$. Each user in the group changes its direction from the general movement vector $\vec{V}^t_{group}$ by a certain degree. Mobility of each user is defined by a reference point that follows the cluster's movement. Nominally, the mobility vector $\vec{V}^t_i$ of a group member i can be described as:

$$\vec{V}^t_i = \vec{V}^t_{group} + \vec{M}^t_i, \tag{4.1}$$

where $\vec{V}^t_{group}$ is the vector of the group center movement and $\vec{M}^t_i$ is the random deviation vector for the group member i.

Group trajectories employ the random direction mobility (RDM), while vector $\vec{M}^t_i$ follows independent and identically distributed (i.i.d.) random variables. Its length is distributed uniformly within a determined radius $[0, d_{max}]$ centered at the reference point, where d_{max} is the maximum allowed distance variation, whose direction is distributed uniformly over the interval $[0, 2\pi]$.

By appropriate choice of points and parameters in the RPGM model, it is possible to characterize various mobility applications. In this context, several applications of the RPGM model can be simulated [46]. For example, RPGM includes the 'geographical

partition model', where the entire space is divided into adjacent areas with a different group in each area. This model can be used for a large-scale situation, where different teams work in their dedicated regions. Another application can be 'overlapped operation', where different groups carry out various tasks over the same area. The next application is a 'convention scenario'. It models the interaction between exhibitors and attendees. For example, in this scenario, several groups may demonstrate their products in separate but connecting areas. A group of attendees travels from area to area, and they may stop in one area for a while and then move on to another. Alternatively, the group may pass through one zone instantly.

4.3 Particle Swarm Optimization

For the purposes of UAV-based IAB optimization, we consider a dedicated dynamic algorithm based on particle swarm optimization (PSO) method. PSO is a useful heuristics that addresses dynamic optimization by iteratively improving a solution with respect to a given parameter. This algorithm emulates the interactions between particles to share information. It solves the problem by having a set of possible solutions in the feasible region of a given problem. The movement of each particle is influenced by its local best-known position but is also guided toward the best-known positions in the search space, which are updated as better positions are being discovered by other particles.

Particle swarm optimization is a stochastic optimization algorithm. The ultimate purpose of the invention of this optimization algorithm was on the modeling of animals social behavior. The group behavior of various animals such as birds or fishes falls under a certain pattern, which inspired the authors of the algorithm to develop it. The approach preserves a swarm of particles, where each particle is a possible solution to the current problem. A cost function is employed in the search space to measure the accuracy of particles. Initially, the particles are distributed randomly across the search area of interest, then they are adjusted according to their personal experience and knowledge of the best particle position of the swarm.

Furthermore, particle swarm optimization is a metaheuristic approach. Metaheuristics usually do not ensure the finding of an optimal solution. Besides, the algorithm does not employ the gradient of the problem under consideration, meaning that it does not demand that the optimization problem be differentiable as is required by traditional optimization methods [47].

The idea of the method can be graphically described as in Fig. 4.4. For particle i, the position of the particle is denoted as $\vec{x}_i$. To distinguish between steps, t shows the iteration number of the algorithm. Also, every particle has a velocity, which describes the movement of particle i in the sense of direction in the search space. In addition to the position and velocity, every particle has a memory of its own best position, where it has the best solution. This is denoted as a personal best $\vec{p}_i$. Moreover, in addition to the personal

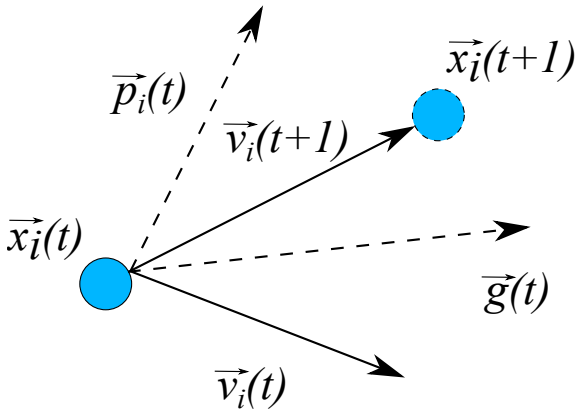

Figure 4.4. *Basic idea of the PSO algorithm.*

best, global best experience exists among all particles, denoted as $\vec{g}$. In contrast, the global best experience belongs to the whole swarm. The new position $\vec{x}_i(t+1)$ is created accordingly to the previous velocity, personal best and global best solutions. Therefore, the particle is moving to a new position using the three vectors. Mathematically it can be described as follows:

$$\begin{cases} \vec{v}_i(t+1) = w \cdot \vec{v}_i(t) + c_1 \cdot (\vec{p}_i(t) - \vec{x}_i(t)) + c_2 \cdot (\vec{g}(t) - \vec{x}_i(t)) \\ \vec{x}_i(t+1) = \vec{x}_i(t) + \vec{v}_i(t+1), \end{cases} \tag{4.2}$$

where $\vec{v}_i(t)$ is the velocity of the particle, $\vec{p}_i$ is the personal best solution, $\vec{g}$ is the global best solution, and parameters w, c_1, and c_2 are selected by the practitioner and control the behavior and efficiency of the PSO method. Example result of the PSO algorithm is presented in the Fig. 4.5b.

The suggested algorithm is shown in Algorithm 1.

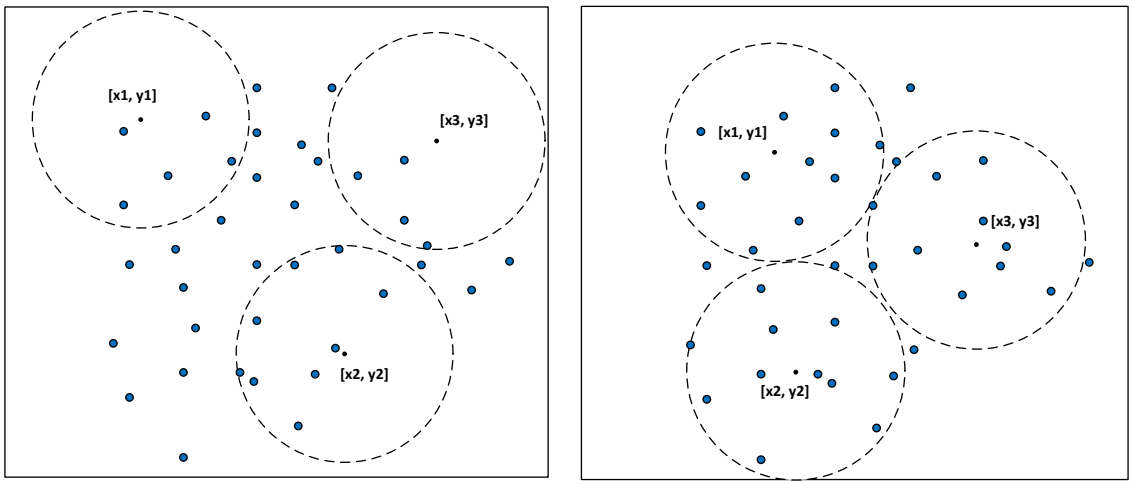

(a) *Initial positions* ***(b)*** *PSO algorithm's result*

Figure 4.5. *Example of the PSO algorithm.*

Algorithm 1. *PSO algorithm for the UAV-BSs placement*

Create a group containing N random particles $X^{(n)}(0), n = 1, \ldots, N$.
Set the dimension of each particle to $M \times 3$.
Set $i = 1$, $Q^{(global)}$=$max\{Q^{(n)}(0, n = 1, \ldots, N)\}$
while $Q^{(global)} < L$ **do**
  for $l = 1, \ldots, N$ **do**
    Calculate $V^{(n)}(i), X^{(n)}(i), Q^{(n)}(i)$
    if $Q^{(n)}(i) > Q^{(n,local)}(i)$ **then**
      $X^{(n,local)} = X^{(n)}(i), Q^{(n,local)} = Q^{(n)}(i)$
      if $Q^{(n,local)} > Q^{(global)}$ **then**
        $X^{(global)} = X^{(n,local)}$,
        $Q^{(global)} = Q^{(n,local)}$
      end if
    end if
    $i = i + 1$
  end for
end while

4.4 Simulation Approach and Metrics

Modern cellular communication systems are one of the most complex segments in the telecom sector. New solutions and mechanisms are being developed and integrated into cellular systems. Therefore, the analysis of such comprehensive structures requires advanced tools and resources. To access the overall performance, system-level simulation (SLS) tools are typically employed. The prior goal of such system-level simulators is to predict how the real-world network will operate under certain conditions. This approach enables to avoid building, validating, and testing a real network. Instead, the cellular network may be evaluated indirectly and system parameters may be tuned according to the purpose. Otherwise, a network operator may lose a tremendous amount of resources after the network configuration.

In this work, the numerical assessment is conducted with our custom-made system-level simulator named WINTERsim, which has been utilized extensively for 5G/5G+ performance evaluation [43]. This simulation environment was further extended to support UAV-BSs in accordance with the recent 3GPP requirements on aerial access (see TR 38.874). The example of PSO-based and grid deployments are shown in Fig. 4.6. The modeler is based on a discrete-event simulation framework. The statistics are collected during the steady-state period by using the method of batch means – via sampling the state of the system every second of simulation time. The beginning of the steady-state period is determined with an exponentially-weighted moving average test where the smoothing constant is set to 0.05.

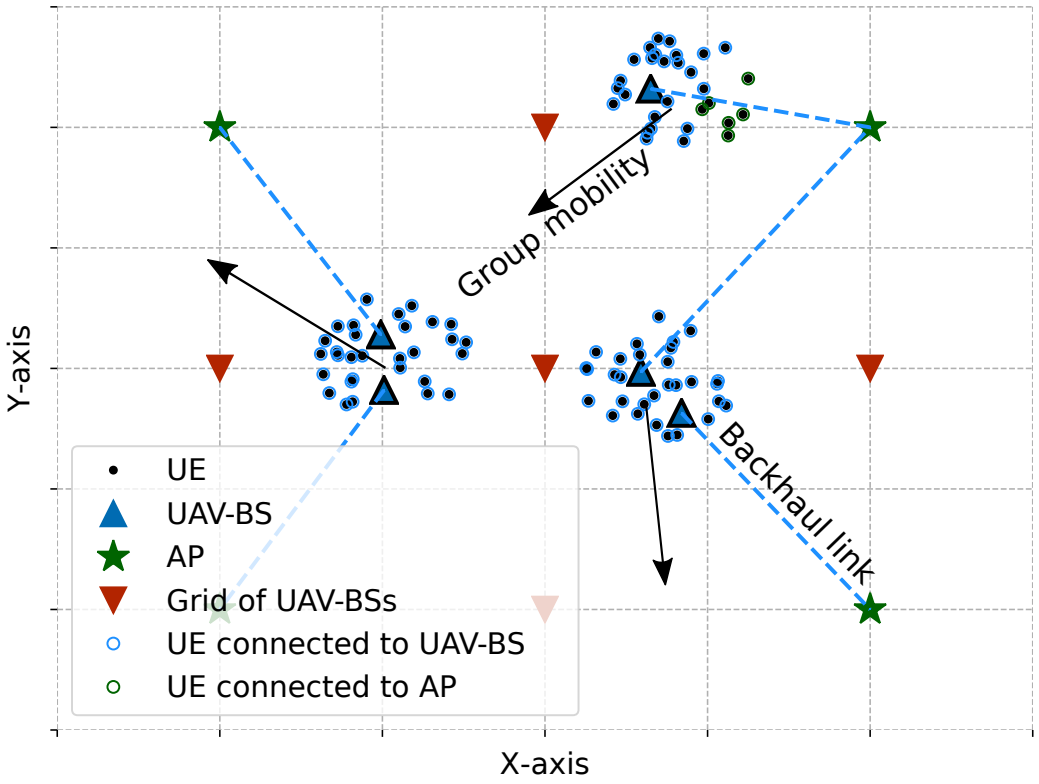

Figure 4.6. *Example of PSO-based and grid deployment of UAV-BSs.*

In the WINTERsim system-level simulator, a UE measures signal strength continuously (with a certain time interval) and independently for each BS, which it can detect. Therefore, one of the important features of the simulator is the physical layer measurements supported by path loss, interference, and multipath fading models. There are also auxiliary functionalities, which include active antenna arrays, various antenna models, and beam sweeping.

We consider two metrics of interest: the mean UE throughput and fairness. For the latter, we use the Jain's fairness index, which quantifies the "equality" of UE performance:

$$J(x_1, x_2, \ldots, x_n) = \frac{(\sum_{i=1}^{n} x_i)^2}{n \cdot \sum_{i=1}^{n} x_i^2}, \tag{4.3}$$

where x_i is the throughput for the ith connection, n is the number of users. If all the UEs receive the same throughput, this index equals 1.

Jain's fairness index is one of the most popular metrics to capture resource distribution variance in wireless networking. One can also use, for example, a combination of the 5-percentile, 95-percentile, and mean value, but Jain's index is easier and is normally more representative. Assuming the values from zero to one, the Jain's index demonstrates fairness regardless of the total network capacity. Typically, the fairness performance of a

wireless network depends on three factors: UEs and BSs positions, the environment in terms of channel conditions, and MAC scheduler implementations. The MAC scheduler can be used to compensate for variations of the first two factors, by offering more resources to the user with poor connectivity, which introduces a trade-off between the total network capacity and fairness.

5 NUMERICAL RESULTS AND ANALYSIS

In this section, we explore the performance of UAV-based IAB systems in urban deployments with clustered mobile users. Particularly, we demonstrate the gains of utilizing optimized UAV-based IAB operation over the conventional grid deployment as well as characterize the trade-offs arising from converged aerial and terrestrial communications.

5.1 Performance of Validation Scenarios

To adjust the simulation framework, we have started with a configuration setup of straightforward scenarios in SLS: the scenarios include one infrastructure AP, one UAV-BS, and UEs distributed over the area of interest (Fig. 5.1). The goal of these simulations is the finding of optimal values of variable parameters.

Our initial scenarios include the following cases:

- In the first scenario, we consider the case, where a UAV-BS always hovers over the center of the UE cluster. We assume that the altitude of the UAV-BS is fixed, and it alters its direction solely in a horizontal plane. In what follows, we vary the distance from the UAV-BS, and consequently the UE cluster, to the ground AP.
- Another scenario considers a similar deployment. However, in this case, 2D distance from the UAV-BS to the AP is fixed, and the variable parameter is the altitude of the UAV-BS. Also, we assume that each time the coverage radius of the UAV is changed, the radius of the UE cluster is also changed correspondingly.
- In the third scenario, the distance from the center of the cluster of UEs to the ground AP is fixed, the radius of the UE cluster and the altitude of the UAV-BS are fixed as well. The only changing parameter is the position of the UAV-BS, it moves between the center of the UE cluster and the ground AP.

Fig. 5.2 shows the data throughput of access and backhaul links for different distances between ground AP and UAV-BS. We have observed that the throughput of access link remains unchanged since UAV-BS always hovers over the cluster of UEs. On the contrary, the overall throughput of backhaul link decreases with increasing distance from the AP.

Fig. 5.3 shows the data throughput of access and backhaul links for different altitude of UAV-BS. It can be seen that the throughput of backhaul and access links decrease with increasing altitude. Since we consider aggregated data traffic from UEs, which is buffered

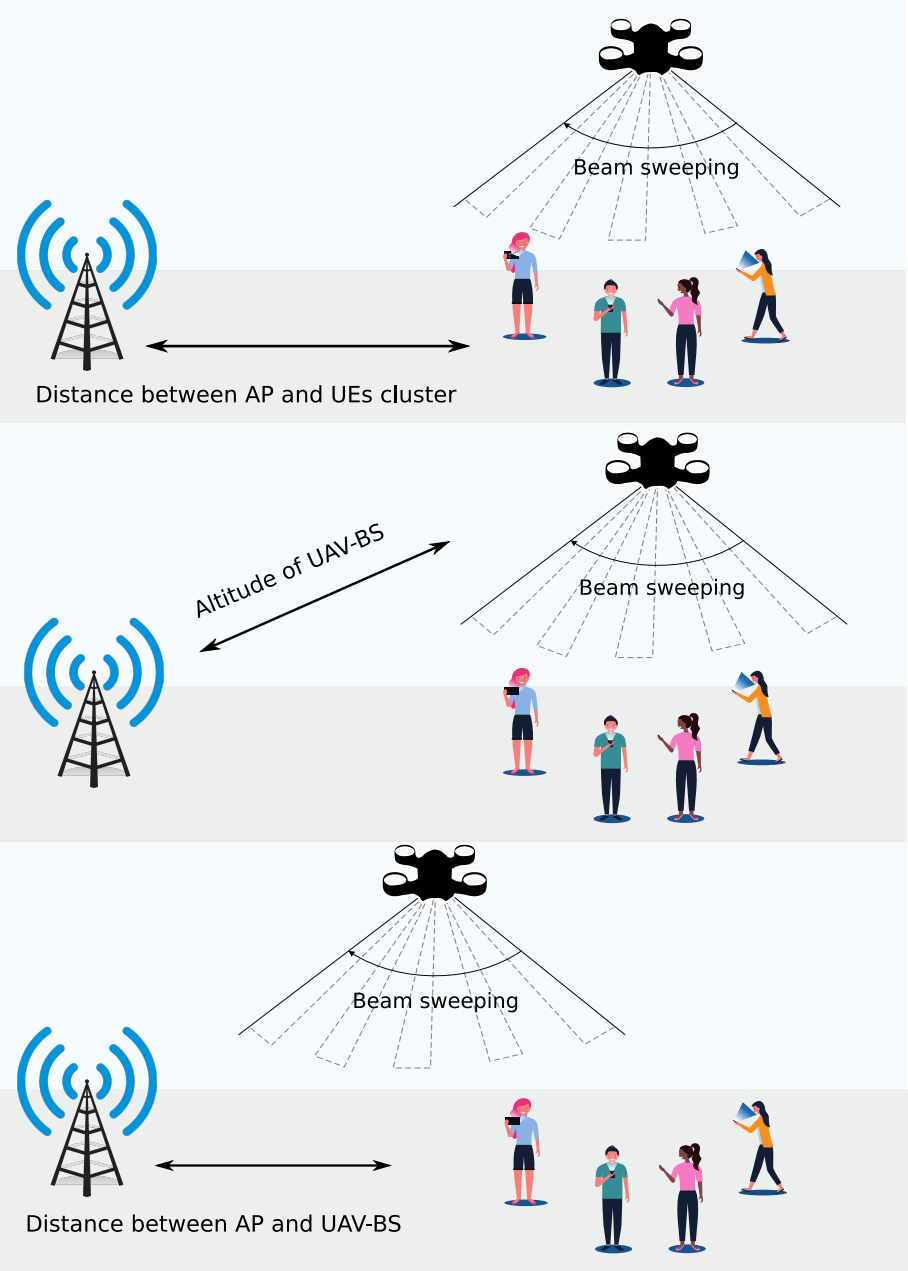

Figure 5.1. *Illustration of the simulated scenarios.*

at the UAV-BS, backhaul link throughput cannot exceed the access link's one. Therefore, the access link is a bottleneck, which confines the overall data rate.

Fig. 5.4 shows the data throughput of access and backhaul links for different distances between ground AP and UAV-BS. We have observed that throughput of the access link grows with increasing distance from AP to UAV-BS, since the deployment of UEs is fixed. By contrast, the throughput of the backhaul link drops with increasing distance. However, due to the fact that access data rate is aggregated at the UAV-BS, backhaul throughput is limited by access link.

Overall, the results of these scenarios are throughput values for backhaul and access links. These elementary scenarios helped to find the optimal cost function for the opti-

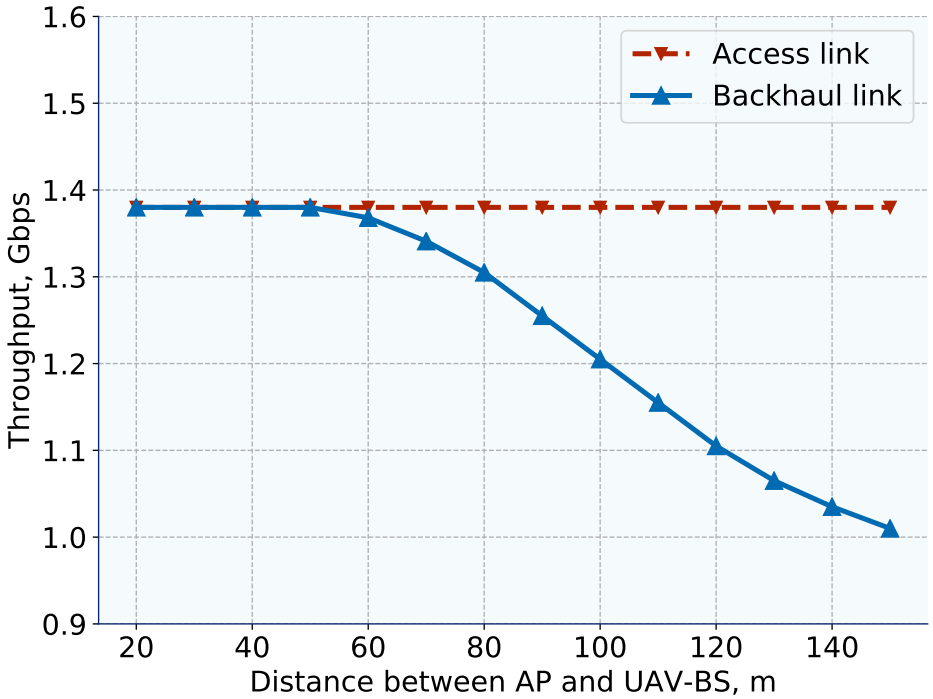

Figure 5.2. *Throughput dependence for the first scenario.*

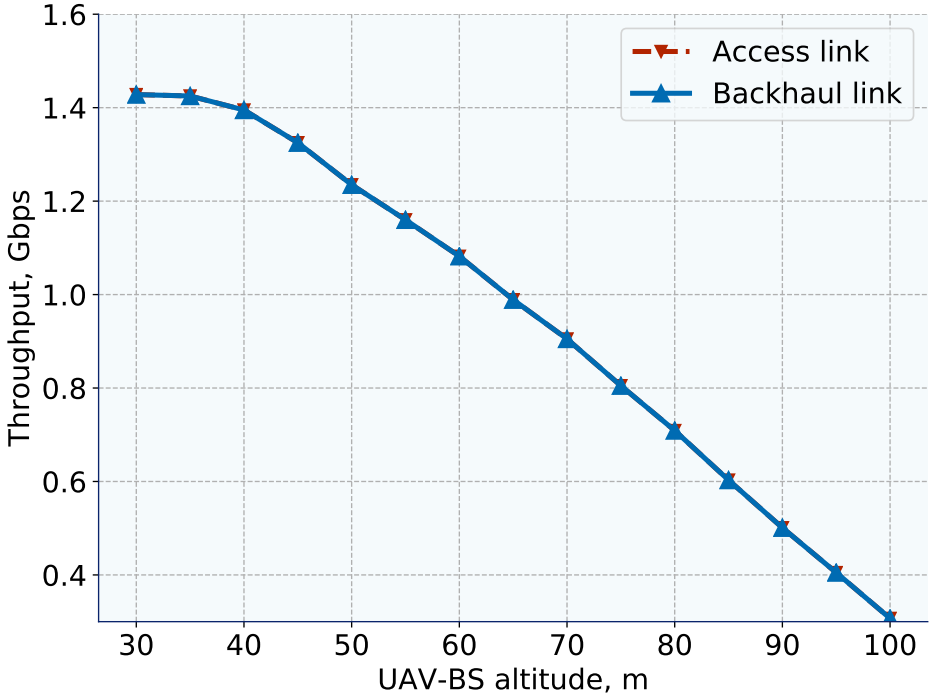

Figure 5.3. *Throughput dependence for the second scenario.*

mization problem. Moreover, the accurate selection of antenna arrays and their parameters is essential for proper system-level simulation. Using the result of the simulations, optimal antenna parameters were obtained. In addition, these scenarios supported simulation framework validation and testing.

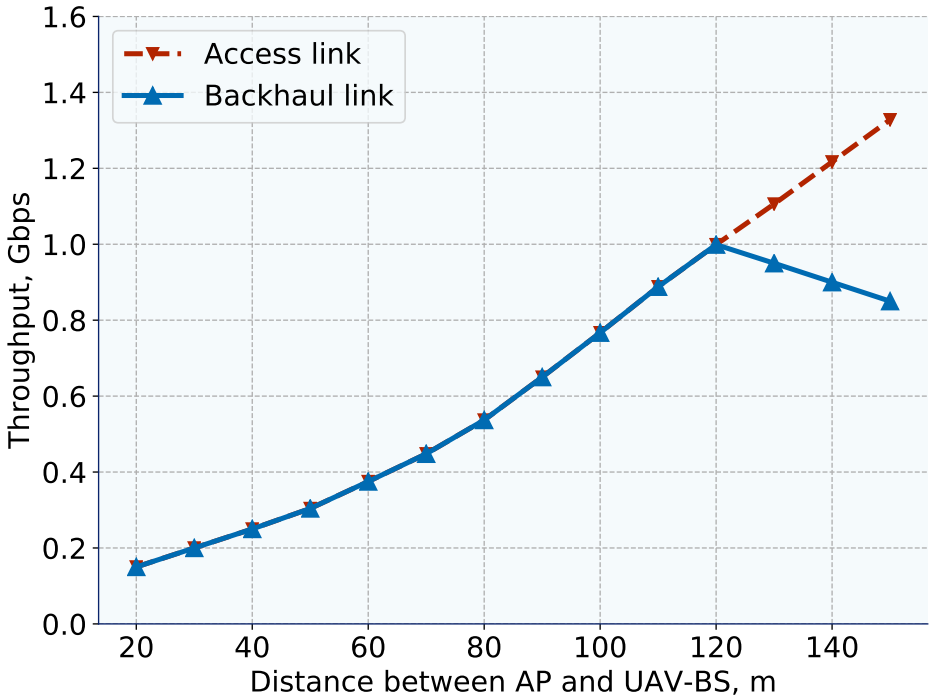

Figure 5.4. *Throughput dependence for the third scenario.*

5.2 Performance of UAV-based IAB Systems

We proceed with providing the representative numerical results for UAV-based IAB operation. We start by highlighting the importance of accounting for constraints imposed by backhauling in the considered integrated terrestrial/aerial deployment. Fig. 5.5 reports on the cumulative distribution function (CDF) of the mean UE throughput for the considered dynamic PSO optimization algorithm in three different cases: (i) ideal backhaul, (ii) backhaul-unaware, and (iii) backhaul-aware. The former assumes that the backhaul bandwidth is not limited and may potentially accommodate all the requirements imposed by the UEs at the UE-UAV interface. In the backhaul-unaware scheme, we enforce a backhaul bandwidth rate limitation but it is not accounted for by the optimization algorithm. Finally, backhaul-aware scheme explicitly incorporates the rate limitation at the backhaul air interface. Note that the former two assumptions are often adopted in various studies of aerial communications [14].

Analyzing the results in Fig. 5.5, one may observe that the ideal backhaul scheme significantly overestimates the actual throughput, since the probability of having the throughput of less than about 0.7 Gbps is negligibly small. This is explained by the fact that all of the traffic generated by the UEs in the UAV-BS coverage areas is assumed to be delivered to the APs successfully. This assumption allows the optimization algorithm to position the UAV-BSs directly on top of the user clusters, thus maximizing the throughput at the UE-UAV air interface. Conversely, the backhaul-unaware scheme drastically underestimates the actual throughput, as it does not explicitly account for the backhaul rate limitation. In

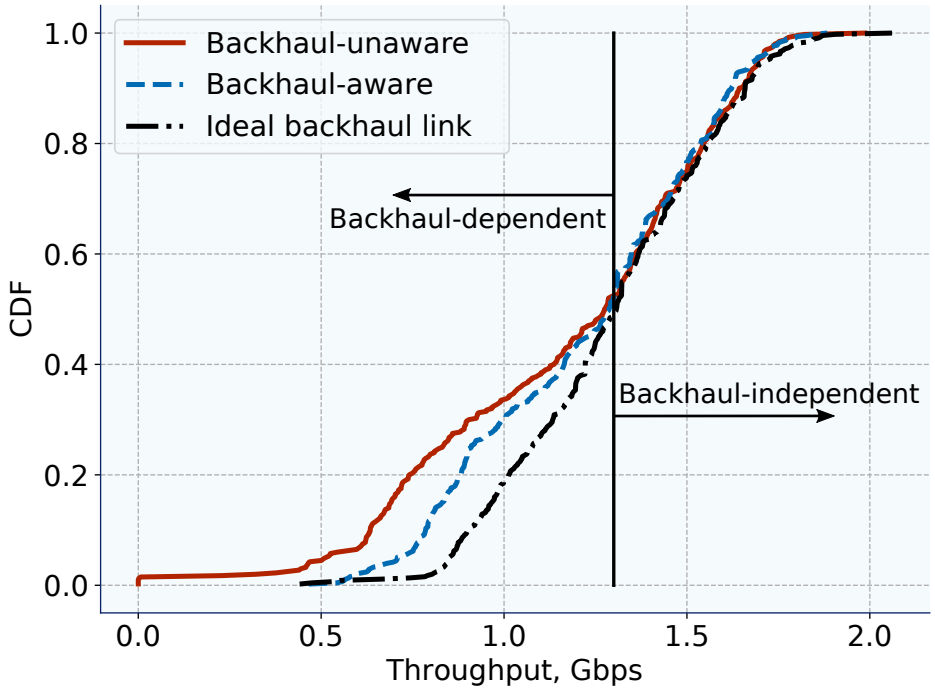

Figure 5.5. *CDF of backhaul throughput.*

this case, the UAV-BSs are positioned similarly to those in the ideal backhaul case but the rate at the UAV-AP interface is often insufficient to offload all of the generated traffic. Here, the system operates in its backhaul-limited regime. The system parameters are summarized in Table 5.1.

Finally, when explicitly accounting for both access and backhaul limitations, the actual throughput is in-between the above two extremes. In this case, the positions of the UAV-BSs are no longer selected on top of the cluster centers, since the higher backhaul rate requirement shifts them closer to the currently associated AP. Another interesting observation in Fig. 5.5 is that the performance of all the considered schemes differs only for low-to-medium throughput allocations, which means that starting from approximately 1.3 Gbps the curves coincide with each other. This is a consequence of having the throughput limitations on the backhaul links. In particular, the throughput of the best-located AP is the same in all of the cases, which yields that for the cluster of UEs deployed close to the AP the backhaul link does not have much impact.

It is natural to expect that the UAV-BS positions and thus the UE throughput allocations will heavily depend on the interplay between the number of clusters and the number of UAV-BSs. We study this effect by using the mean UE throughput as our parameter of interest. In Fig. 5.6, we vary the number of UAV-BSs deployed in the scenario while keeping the number of clusters equal to 4. This graph also compares the results for the dynamic PSO-based algorithm with those for the static grid-based deployment of the UAV-BSs. As expected, for both deployments the mean UE throughput increases as the number of UAV-BSs grows. The most significant difference between the deployments

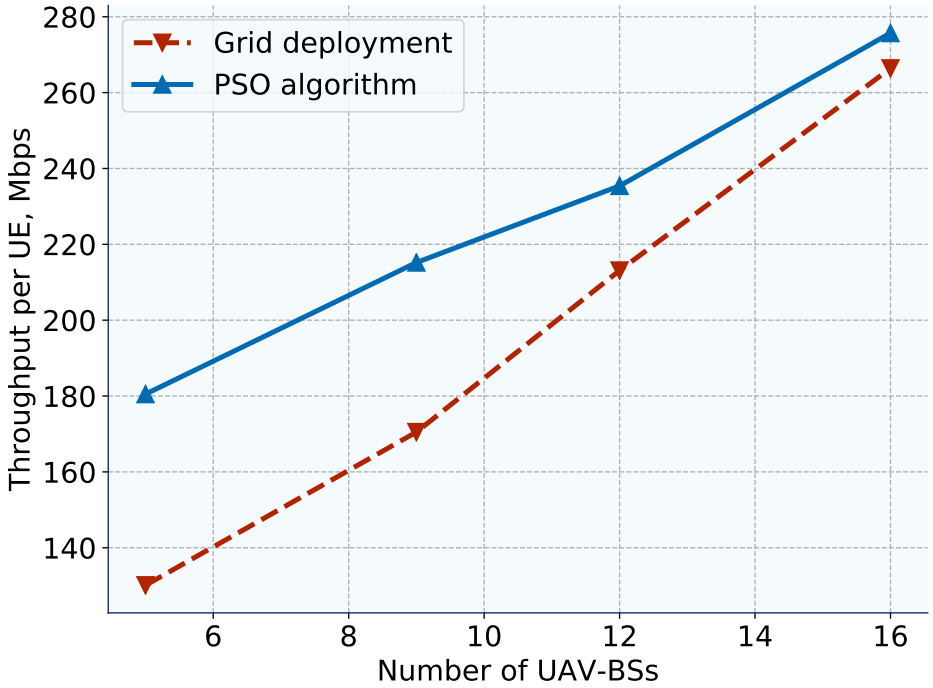

Figure 5.6. *Mean UE throughput for different numbers of UAV-BSs.*

is observed for a small number of UAV-BSs. The system parameters for this case are summarized in Table 5.2.

The rationale behind this behavior is that here the grid-based deployment cannot fully serve the area of interest, and occasionally the UEs either end up far away from the UAV-BSs or may not be under their coverage. As the number of nodes increases, this difference decreases, since the grid-based deployment now densely spans across the entire service area and all of the UEs are always within coverage of at least one UAV-BS.

Another reason for the reduced gains is that with an extremely high number of UAV-BSs the interference starts to play an important role for the achievable throughput by not allowing the algorithm to position the UAV-BSs as close as needed. This can be alleviated with the use of more directional antennas at the UEs by efficiently isolating the UE transmissions to the closely located UAV-BSs. However, even for these highly dense deployments, the use of dynamic optimization techniques allows for improved UE throughputs by optimally positioning the UAV-BSs around the UE clusters and following these clusters at all times.

The considered dynamic PSO algorithm is useful for determining the optimized UAV-BS locations to maximize the UE throughput based on the α-fairness criterion. In Fig. 5.7, we study the impact of the number of clusters on the Jain's fairness index by keeping the number of UAV-BSs constant at 5 for the two considered UAV-BS deployments. The system parameters are summarized in Table 5.3. First, it is important to note that an increase in the number of UE clusters leads to a drop of fairness between the throughput allocations. Particularly, there is a significant degradation for three clusters. The under-

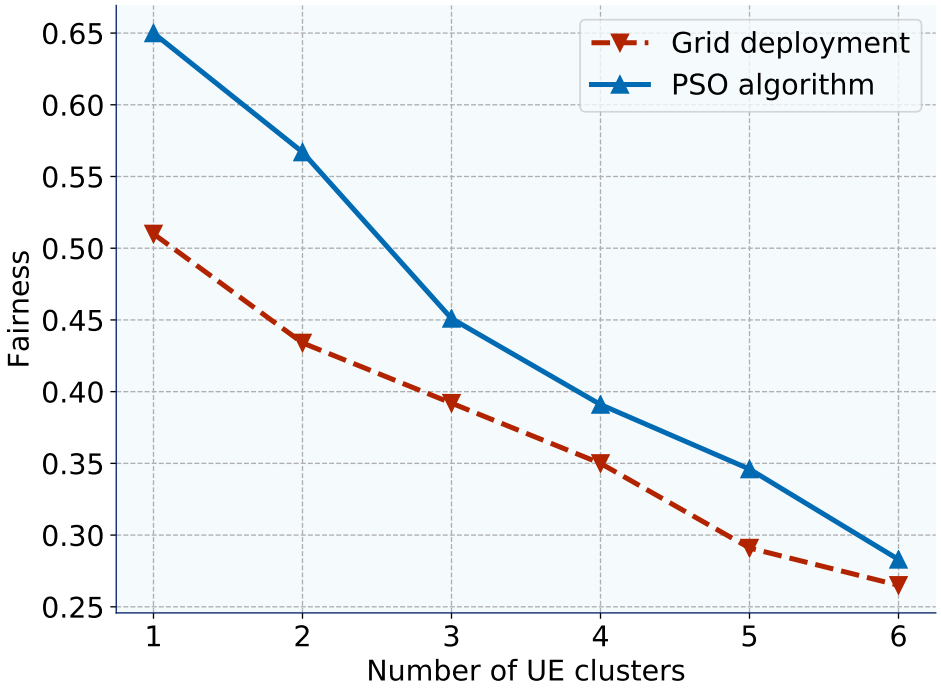

Figure 5.7. *Fairness for different numbers of UE clusters.*

lying reason for this in case of dynamic PSO optimization is that for one, two, or four clusters there are distinct ”optimal” combinations of the UAV-BS positions, which lead to similar UE performance.

For example, for four UAV-BSs and two UE clusters the PSO algorithm forces the UAV-BSs to track the clusters residing on their opposite sides (two UAV-BSs per cluster). Hence, the available UE throughput is almost equal and the only difference comes from random UE locations inside the clusters. As the number of clusters increases, there are no such positions, which result in equal distances to the associated UAV-BSs. In other words, the said algorithm attempts to split the UAV-BSs fairly between the clusters, but in case of, e.g., three clusters and five UAV-BSs, there will be one cluster served solely by a single UAV-BS; hence, the Jain's fairness index degrades. For the grid-based deployment, one may observe a similar trend – the fairness of UE throughput allocations decreases. However, this trend is milder, since for an increase in the number of clusters the fraction of out-of-coverage UEs decreases, which contributes positively to the Jain's fairness index.

Similarly to Fig. 5.6, the highest gains in fairness are achieved for a small number of UE clusters, that is, in case of one or two clusters. Already for three clusters, the fairness values for the two deployment schemes become close to each other. Even though the PSO-based solution still demonstrates a better performance, the UAV-BS grid is composed in a way that maximizes the probability for the UEs to be covered by at least one UAV-BS or a ground AP.

The performance levels of the two considered deployments become ever more similar

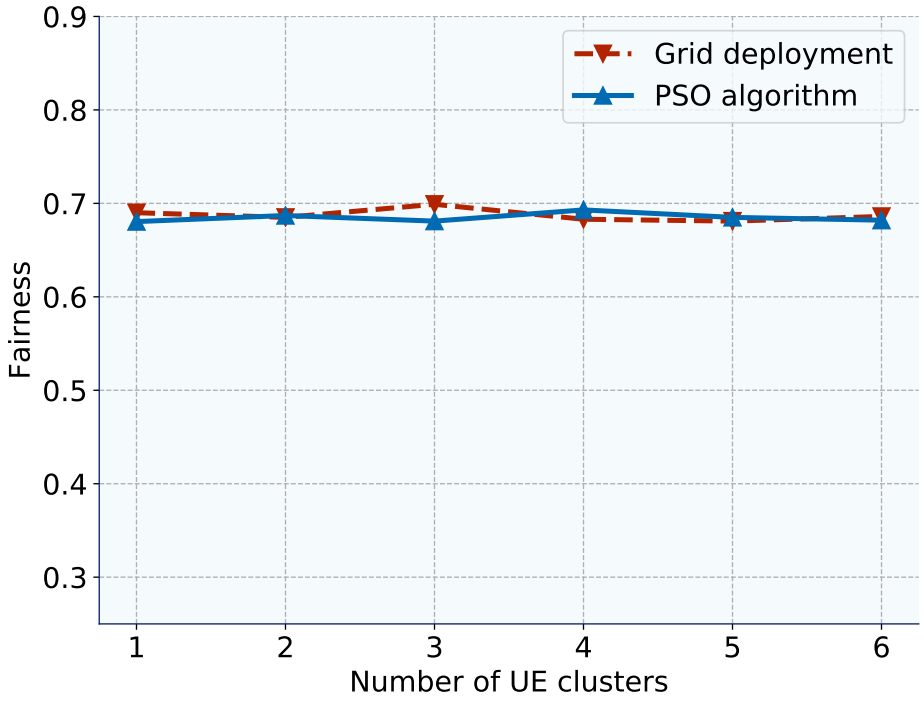

Figure 5.8. *Fairness for different numbers of UE clusters.*

when the number of clusters is higher than the number of UAV-BSs (i.e., six and five in our scenario, respectively). In that case, the algorithm in question will aim to place one of the UAV-BSs in-between the two clusters to provide at least some coverage, but it may not be possible due to long distance between the clusters. Accordingly, the UEs of the isolated cluster will need to rely solely upon the ground network, and the fairness performance will remain similar to that of the grid deployment.

In this work, we set the scheduler as Round-Robin, which distributes resources equally regardless of the channel conditions and introduces an additional degree of freedom by allowing for UAV-BS mobility. As it is shown previously, when the UAV-BSs cannot cover the entire service area, the UAV-BS mobility allows not only to increase the network capacity but also to improve fairness and thus avoid the aforementioned capacity-to-fairness trade-off. Although the fairness may drop if one decreases the number of deployed UAV-BSs, the PSO algorithm still allows performing better than the static UAV-BS deployment.

To show the values of fairness, we have modeled a similar scenario where the number of UAV-BSs is equal to 16. Fig. 5.8 reports the fairness index for different numbers of UE clusters. As one may observe, an increase in the number of UE clusters does not lead to a decrease in the fairness index as compared to the case with 5 UAV-BSs. This can be explained by the fact that the deployment of 16 UAV-BSs fully covers the area of interest. Therefore, end-users acquire approximately equal resources regardless of the number of UE clusters. Similarly, the PSO algorithm handles 16 UAV-BSs over a fewer number of UE clusters, and, thus, UAV-BSs are able to equally divide the resources.

Table 5.1. *Modeling Parameters for the First Scenario.*

Parameter	**Value**
Deployment area	600 m x 600 m
Number of APs	4
Number of UAV-BSs	2
Number of UEs	100
Distribution of UEs	Clustered
Radius of UE distribution	50 m
Seeds	200
Channel model for AP-UAV link	mmWave Channel Model LOS [48]
Channel model for AP-UE link	mmWave Channel Model [48]
Channel model for UAV-UE link	mmWave Channel Model [48]
AP planar antenna arrays	8x8 (access and backhaul)
UAV-BS planar antenna arrays	8x8 (access), 4x4 (backhaul)
UAV-BS altitude	20 m
AP height	20 m
UE height	1.5 m
Carrier frequency	73 GHz [32]
System bandwidth	0.56 GHz [32]
Transmit power	24 dBm
Power control	Full-power
Beam-sweeping periodicity	3 μs
Frame size	3 μs
Transmission mode	TDM
Packet size	1000 bytes
Target data rate	500 Mb/s
AP and UAV-BS scheduling	Round-Robin
Value of α	2

Table 5.2. *Modeling Parameters for the Second Scenario.*

Parameter	**Value**
Deployment area	600 m x 600 m
Number of APs	4
Number of UAV-BSs	5/9/12/16
Number of UEs	100
Distribution of UEs	Clustered
Radius of UE distribution	50 m
Seeds	200
Channel model for AP-UAV link	mmWave Channel Model LOS [48]
Channel model for AP-UE link	mmWave Channel Model [48]
Channel model for UAV-UE link	mmWave Channel Model [48]
AP planar antenna arrays	8x8 (access and backhaul)
UAV-BS planar antenna arrays	8x8 (access), 4x4 (backhaul)
UAV-BS altitude	20 m
AP height	20 m
UE height	1.5 m
Carrier frequency	73 GHz [32]
System bandwidth	0.56 GHz [32]
Transmit power	24 dBm
Power control	Full-power
Beam-sweeping periodicity	3 μs
Frame size	3 μs
Transmission mode	TDM
Packet size	1000 bytes
Target data rate	500 Mb/s
AP and UAV-BS scheduling	Round-Robin
Value of α	2

Table 5.3. *Modeling Parameters for the Third Scenario.*

Parameter	**Value**
Deployment area	600 m x 600 m
Number of APs	4
Number of UAV-BSs	5
Number of UE clusters	1/2/3/4/5/6
Distribution of UEs	Clustered
Radius of UE distribution	50 m
Seeds	200
Channel model for AP-UAV link	mmWave Channel Model LOS [48]
Channel model for AP-UE link	mmWave Channel Model [48]
Channel model for UAV-UE link	mmWave Channel Model [48]
AP planar antenna arrays	8x8 (access and backhaul)
UAV-BS planar antenna arrays	8x8 (access), 4x4 (backhaul)
UAV-BS altitude	20 m
AP height	20 m
UE height	1.5 m
Carrier frequency	73 GHz [32]
System bandwidth	0.56 GHz [32]
Transmit power	24 dBm
Power control	Full-power
Beam-sweeping periodicity	3 μs
Frame size	3 μs
Transmission mode	TDM
Packet size	1000 bytes
Target data rate	500 Mb/s
AP and UAV-BS scheduling	Round-Robin
Value of α	2

6 CONCLUSION

Integrated Access and Backhaul is an emerging technology considered by 3GPP for cellular densification and coverage extension. Future UAV-based IAB systems operating in mmWave spectrum therefore become a promising solution due to their higher data rates at the access and backhaul links, lower interference, and more flexible service dynamics. However, the deployment of such systems is subject to multiple restrictions related to the infrastructure network support, resource partitioning between the access and the backhaul links, as well as correlated mobility of the UEs and UAV-BSs.

In this work, we provided a detailed account of the recent 3GPP activities behind UAV-based IAB systems that operate in mmWave frequencies. We first considered the ongoing and planned 3GPP activities on UAV support in cellular systems. In particular, we reviewed the use cases and challenges of employing UAV communications. Then, we continued by presenting possible IAB architectures and implementation options. Also, we studied the capabilities of underlying NR relays as important technology enablers.

Next, we investigated a difficult problem of deployment and navigation of UAV-BSs in a relatively wide area. Specifically, in an environment with realistic UE mobility across the terrestrial NR layout, we characterized the important factors and trade-offs related to UAV-aided IAB operation. We evaluated the performance of UAV-aided radio systems enabled by IAB capabilities with the use of system-level simulations. Moreover, we showed the impact of UAV-BS backhaul navigation on the system performance by comparing it with the case of ideal backhauling.

- Particularly, we demonstrated that dynamic methodologies that optimize the UAV-BS positions can unlock substantial gains as compared to rigid deployments, especially in clustered UE environment. Our numerical results showed the gains of approximately 0.2 Gbps for the backhaul-aware solution as well as demonstrated that optimization improves the overall system performance.
- It was illustrated that the performance of all the considered schemes differs only for low-to-medium throughput allocations. This can be explained by the fact that at the distances closer to donor-AP, UAV-BSs are able to fully relay the incoming traffic without any significant packet loss.
- We compared the UE throughput allocations for the dynamic PSO-based algorithm and the static grid-based deployment of the UAV-BSs. As can be expected, for both deployments the mean UE throughput increases as the number of UAV-BSs

grows. The most notable variation between the deployments is observed for a small number of UAV-BSs.

- Also, we compared fairness for the dynamic navigation and the static grid-based deployment of the UAV-BSs. It was observed that an increase in the number of UE clusters leads to a drop of fairness between the throughput allocations.

In this context, the constraints imposed by mmWave backhauling become crucial for the effective performance of UAV-based IAB systems. This work proposed a solid approach to optimize the positions of mmWave-based UAV-BS with IAB capabilities. This method may be used by network operators to enhance the overall system performance.

REFERENCES

[1] 5G-FORCE. *5G Finnish Open Research Collaboration Ecosystem*. https://5g-force.org/. Accessed: 2019-10-23.

[2] SwissPost. *Swiss Post drone takes off again for healthcare services*. https://post-medien.ch/en/swiss-post-drone-lost-over-lake-zurich/. Accessed: 2019-10-23.

[3] Wired. *UPS drones are now moving blood samples over North Carolina*. https://www.wired.com/story/ups-matternet-drone-delivery-north-carolina/. Accessed: 2019-10-23.

[4] Bloomberg. *Google Spinoff's Drone Delivery Business First to Get FAA Approval*. https://www.bloomberg.com/news/articles/2019-04-23/alphabet-s-drone-delivery-business-cleared-for-takeoff-by-faa. Accessed: 2019-10-23.

[5] CairnsPost. *Unmanned aerial vehicles: New drone business in Cairns and Far North Queensland set to take off*. https://www.cairnspost.com.au/business/unmanned-aerial-vehicles-new-drone-business-in-cairns-and-far-north-queensland-set-to-take-off/news-story/. Accessed: 2019-10-23.

[6] I. Bor-Yaliniz, M. Salem, G. Senerath and H. Yanikomeroglu. Is 5G Ready for Drones: A Look into Contemporary and Prospective Wireless Networks from a Standardization Perspective. *IEEE Wireless Communications* 26.1 (2019), 18–27.

[7] H. Hellaoui, O. Bekkouche, M. Bagaa and T. Taleb. Aerial Control System for Spectrum Efficiency in UAV-to-Cellular Communications. *IEEE Communications Magazine* 56.10 (2018), 108–113.

[8] S. Sekander, H. Tabassum and E. Hossain. Multi-Tier Drone Architecture for 5G/B5G Cellular Networks: Challenges, Trends, and Prospects. *IEEE Communications Magazine* 56.3 (2018), 96–103. DOI: 10.1109/MCOM.2018.1700666.

[9] Y. Zeng, Q. Wu and R. Zhang. Accessing from the sky: A tutorial on UAV communications for 5G and beyond. *arXiv preprint arXiv:1903.05289* (2019).

[10] A. Fotouhi, H. Qiang, M. Ding, M. Hassan, L. G. Giordano, A. Garcia-Rodriguez and J. Yuan. Survey on UAV cellular communications: Practical aspects, standardization advancements, regulation, and security challenges. *IEEE Communications Surveys & Tutorials* (2019).

[11] M. Mozaffari, W. Saad, M. Bennis, Y. Nam and M. Debbah. A Tutorial on UAVs for Wireless Networks: Applications, Challenges, and Open Problems. *IEEE Communications Surveys Tutorials* 21.3 (2019), 2334–2360. DOI: 10.1109/COMST.2019.2902862.

[12] J. Pokorny, A. Ometov, P. Pascual, C. Baquero, P. Masek, A. Pyattaev, A. Garcia, C. Castillo, S. Andreev, J. Hosek et al. Concept design and performance evaluation

of UAV-based backhaul link with antenna steering. *Journal of Communications and Networks* 20.5 (2018), 473–483.

[13] Y. Zeng, R. Zhang and T. J. Lim. Wireless Communications with Unmanned Aerial Vehicles: Opportunities and Challenges. *IEEE Communications Magazine* 54.5 (2016), 36–42. DOI: 10.1109/MCOM.2016.7470933.

[14] M. Gapeyenko, V. Petrov, D. Moltchanov, S. Andreev, N. Himayat and Y. Koucheryavy. Flexible and Reliable UAV-Assisted Backhaul Operation in 5G mmWave Cellular Networks. *IEEE Journal on Selected Areas in Communications* 36.11 (Nov. 2018), 2486–2496.

[15] N. B. Labs. *Unmanned aerial vehicles: flying cell*. https://www.nokia.com/innovation/nokia-bell-labs/. Accessed: 2019-10-23.

[16] J. Gong, T.-H. Chang, C. Shen and X. Chen. Flight time minimization of UAV for data collection over wireless sensor networks. *IEEE Journal on Selected Areas in Communications* 36.9 (2018), 1942–1954.

[17] P. Zhou, X. Fang, Y. Fang, R. He, Y. Long and G. Huang. Beam management and self-healing for mmWave UAV mesh networks. *IEEE Transactions on Vehicular Technology* 68.2 (2018), 1718–1732.

[18] S. Yin, Y. Zhao and L. Li. UAV-assisted cooperative communications with time-sharing SWIPT. *2018 IEEE International Conference on Communications (ICC)*. IEEE. 2018, 1–6.

[19] N. Zhao, F. Cheng, F. R. Yu, J. Tang, Y. Chen, G. Gui and H. Sari. Caching UAV assisted secure transmission in hyper-dense networks based on interference alignment. *IEEE Transactions on Communications* 66.5 (2018), 2281–2294.

[20] F. Zhou, Y. Wu, R. Q. Hu and Y. Qian. Computation rate maximization in UAV-enabled wireless-powered mobile-edge computing systems. *IEEE Journal on Selected Areas in Communications* 36.9 (2018), 1927–1941.

[21] A. Orsino, A. Ometov, G. Fodor, D. Moltchanov, L. Militano, S. Andreev, O. N. Yilmaz, T. Tirronen, J. Torsner, G. Araniti et al. Effects of Heterogeneous Mobility on D2D-and Drone-Assisted Mission-Critical MTC in 5G. *IEEE Communications Magazine* 55.2 (2017), 79–87.

[22] E. Kalantari, H. Yanikomeroglu and A. Yongacoglu. On the number and 3D placement of drone base stations in wireless cellular networks. *Vehicular Technology Conference (VTC-Fall), 2016 IEEE 84th*. 2016, 1–6.

[23] S. Iellamo, J. J. Lehtomaki and Z. Khan. Placement of 5G drone base stations by data field clustering. *2017 IEEE 85th Vehicular Technology Conference (VTC Spring)*. IEEE. 2017, 1–5.

[24] N. Tafintsev, D. Moltchanov, M. Gerasimenko, M. Gapeyenko, J. Zhu, S.-P. Yeh, N. Himayat, S. Andreev, Y. Koucheryavy and M. Valkama. Aerial Access and Backhaul in mmWave B5G Systems: Performance Dynamics and Optimization. *IEEE Communications Magazine. To appear* (2019).

[25] D. Solomitckii, M. Gapeyenko, V. Semkin, S. Andreev and Y. Koucheryavy. Technologies for efficient amateur drone detection in 5G millimeter-wave cellular infrastructure. *IEEE Communications Magazine* 56.1 (2018), 43–50.

[26] A. Mourad. Self-Backhauling in 5G. *5G-PPP Workshop on 5G RAN Design, Air Interface Design and Integration, Valencia, Spain*. 2016.

[27] M. Polese, M. Giordani, A. Roy, S. Goyal, D. Castor and M. Zorzi. End-to-End Simulation of Integrated Access and Backhaul at mmWaves. *2018 IEEE 23rd International Workshop on Computer Aided Modeling and Design of Communication Links and Networks (CAMAD)*. IEEE. 2018, 1–7.

[28] F. Boccardi, R. W. Heath, A. Lozano, T. L. Marzetta and P. Popovski. Five disruptive technology directions for 5G. *IEEE Communications Magazine* 52.2 (Feb. 2014), 74–80. ISSN: 0163-6804. DOI: 10.1109/MCOM.2014.6736746.

[29] A. Ghosh, T. A. Thomas, M. C. Cudak, R. Ratasuk, P. Moorut, F. W. Vook, T. S. Rappaport, G. R. MacCartney, S. Sun and S. Nie. Millimeter-Wave Enhanced Local Area Systems: A High-Data-Rate Approach for Future Wireless Networks. *IEEE Journal on Selected Areas in Communications* 32.6 (2014), 1152–1163. DOI: 10.1109/JSAC.2014.2328111.

[30] I. A. Hemadeh, K. Satyanarayana, M. El-Hajjar and L. Hanzo. Millimeter-Wave Communications: Physical Channel Models, Design Considerations, Antenna Constructions, and Link-Budget. *IEEE Communications Surveys & Tutorials* 20.2 (Secondquarter 2018), 870–913. DOI: 10.1109/COMST.2017.2783541.

[31] L. Zhang, H. Zhao, S. Hou, Z. Zhao, H. Xu, X. Wu, Q. Wu and R. Zhang. A Survey on 5G Millimeter Wave Communications for UAV-Assisted Wireless Networks. *IEEE Access* 7 (2019), 117460–117504. DOI: 10.1109/ACCESS.2019.2929241.

[32] T. S. Rappaport, Y. Xing, G. R. MacCartney, A. F. Molisch, E. Mellios and J. Zhang. Overview of millimeter wave communications for fifth-generation (5G) wireless networks—with a focus on propagation models. *IEEE Transactions on Antennas and Propagation* 65.12 (2017), 6213–6230.

[33] M.-H. Golbon-Haghighi. Beamforming in wireless networks. *Towards 5G Wireless Networks-A Physical Layer Perspective*. InTech, 2016.

[34] W. Lee, S.-R. Lee, H.-B. Kong and I. Lee. 3D beamforming designs for single user MISO systems. *Global Communications Conference (GLOBECOM), 2013 IEEE*. IEEE. 2013, 3914–3919.

[35] S. M. Razavizadeh, M. Ahn and I. Lee. Three-dimensional beamforming: A new enabling technology for 5G wireless networks. *IEEE Signal Processing Magazine* 31.6 (2014), 94–101.

[36] E. Yaacoub and Z. Dawy. A survey on uplink resource allocation in OFDMA wireless networks. *IEEE Communications Surveys & Tutorials* 14.2 (2012), 322–337.

[37] R. Kovalchukov, A. Samuylov, D. Moltchanov, A. Ometov, S. Andreev, Y. Koucheryavy and K. Samouylov. Modeling three-dimensional interference and SIR in highly directional mmWave communications. *GLOBECOM 2017*. IEEE. 2017.

[38] M. Gapeyenko, A. Samuylov, M. Gerasimenko, D. Moltchanov, S. Singh, M. R. Akdeniz, E. Aryafar, N. Himayat, S. Andreev and Y. Koucheryavy. On the Temporal Effects of Mobile Blockers in Urban Millimeter-Wave Cellular Scenarios. *IEEE Transactions on Vehicular Technology* 66.11 (Nov. 2017), 10124–10138. DOI: 10.1109/TVT.2017.2754543.

[39] A. Samuylov, M. Gapeyenko, D. Moltchanov, M. Gerasimenko, S. Singh, N. Himayat, S. Andreev and Y. Koucheryavy. Characterizing Spatial Correlation of Blockage Statistics in Urban mmWave Systems. *2016 IEEE Globecom Workshops (GC Wkshps)*. Dec. 2016, 1–7. DOI: 10.1109/GLOCOMW.2016.7848859.

[40] N. Tafintsev, M. Gerasimenko, D. Moltchanov, M. Akdeniz, S.-P. Yeh, N. Himayat, S. Andreev, Y. Koucheryavy and M. Valkama. Improved Network Coverage with Adaptive Navigation of mmWave-Based Drone-Cells. *2018 IEEE Globecom Workshops (GC Wkshps)*. IEEE. 2018, 1–7.

[41] W. Shi, J. Li, W. Xu, H. Zhou, N. Zhang, S. Zhang and X. Shen. Multiple Drone-Cell Deployment Analyses and Optimization in Drone Assisted Radio Access Networks. *IEEE Access* 6 (2018), 12518–12529.

[42] A. E. Eiben, J. E. Smith et al. *Introduction to evolutionary computing*. Vol. 53. Springer, 2003.

[43] M. Gerasimenko, D. Moltchanov, R. Florea, S. Andreev, Y. Koucheryavy, N. Himayat, S.-P. Yeh and S. Talwar. Cooperative radio resource management in heterogeneous cloud radio access networks. *IEEE Access* 3 (2015), 397–406.

[44] T. Camp, J. Boleng and V. Davies. A survey of mobility models for ad hoc network research. *Wireless communications and mobile computing* 2.5 (2002), 483–502.

[45] F. Bai and A. Helmy. A survey of mobility models. *Wireless Adhoc Networks. University of Southern California, USA* 206 (2004), 147.

[46] X. Hong, M. Gerla, G. Pei and C.-C. Chiang. A group mobility model for ad hoc wireless networks. *Proceedings of the 2nd ACM international workshop on Modeling, analysis and simulation of wireless and mobile systems*. Vol. 53. 1999, 60.

[47] Y. Zhao, Y. Chen, R. Jian and L. Yang. A Resource Allocation Scheme for SDN-Based 5G Ultra-Dense Heterogeneous Networks. *2017 IEEE Globecom Workshops (GC Wkshps)*. 2017, 1–6. DOI: 10.1109/GLOCOMW.2017.8269193.

[48] T. A. Thomas, H. C. Nguyen, G. R. MacCartney and T. S. Rappaport. 3D mmWave Channel Model Proposal. *2014 IEEE 80th Vehicular Technology Conference (VTC2014-Fall)*. Sept. 2014, 1–6. DOI: 10.1109/VTCFall.2014.6965800.

A FLOWCHART OF THE PSO ALGORITHM

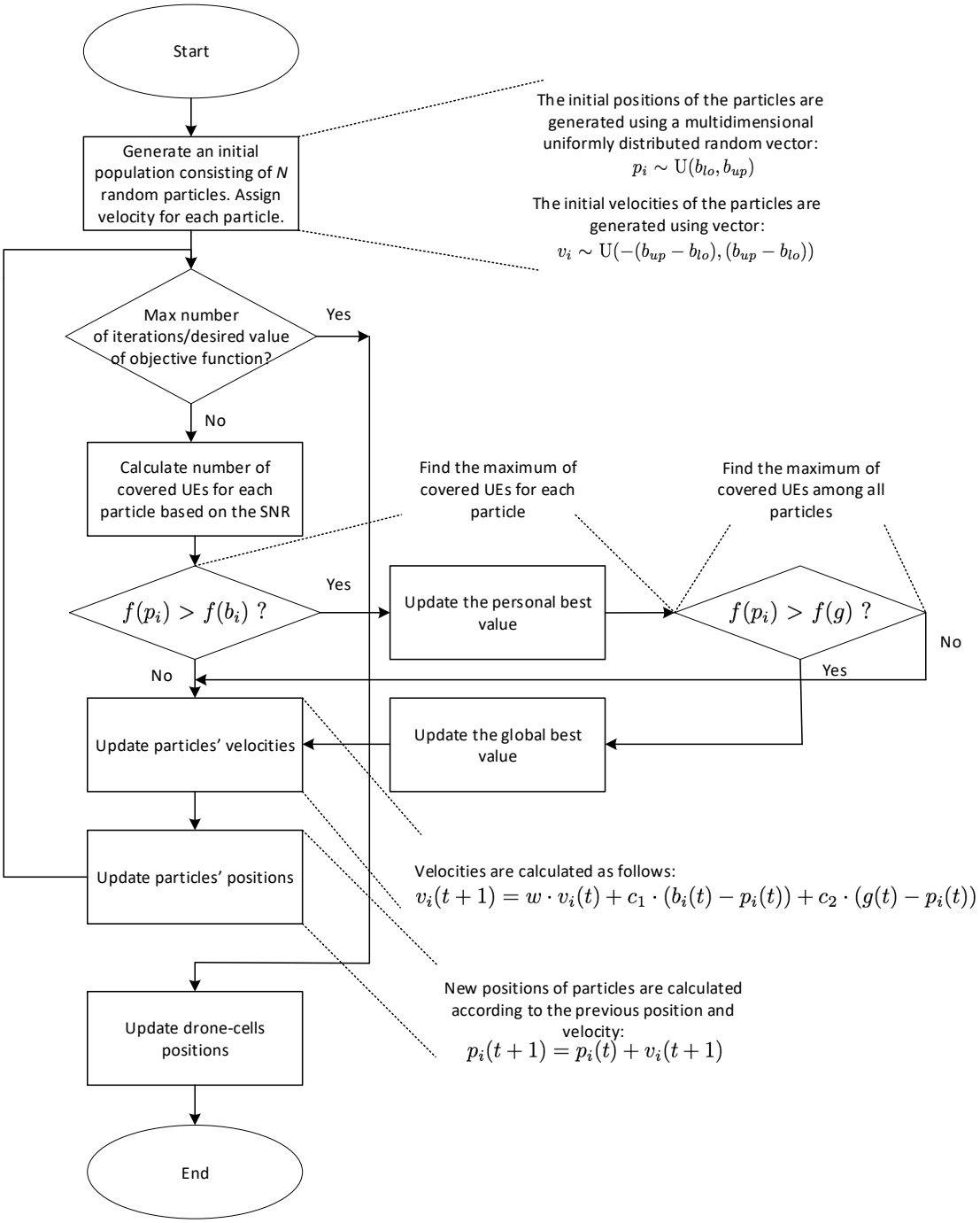

Figure A.1. *Flowchart of the PSO algorithm.*

B VARIOUS PSO-BASED AND GRID-BASED DEPLOYMENTS

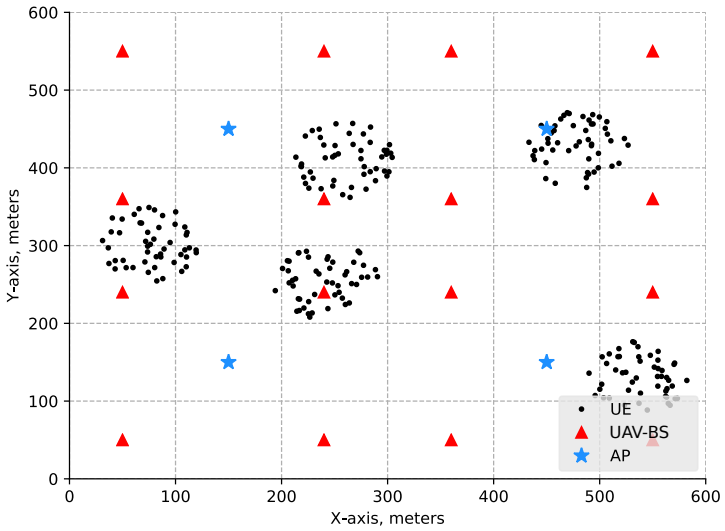

Figure B.1. *Grid-based deployment of 16 UAV-BSs.*

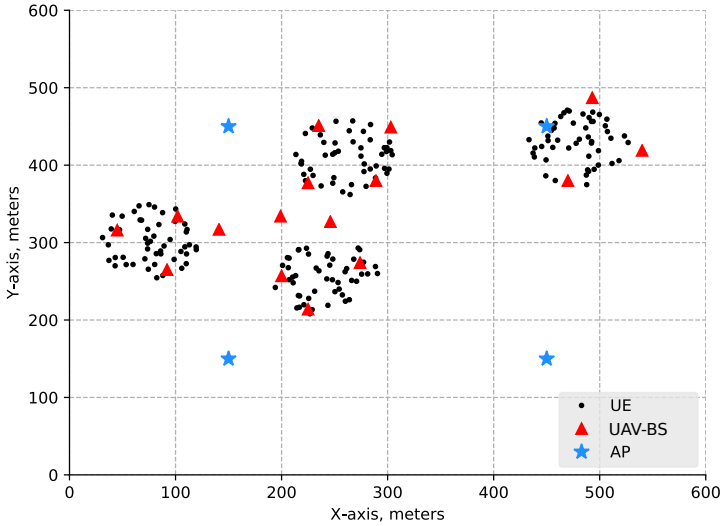

Figure B.2. *PSO-based deployment of 16 UAV-BSs.*

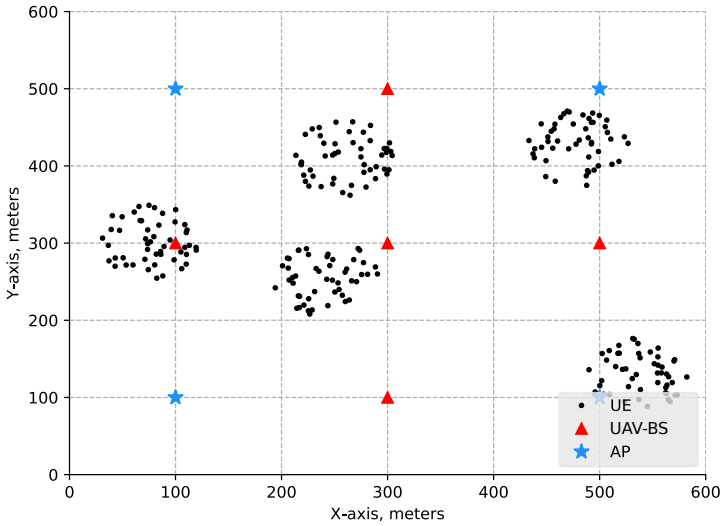

Figure B.3. *Grid-based deployment of 5 UAV-BSs.*

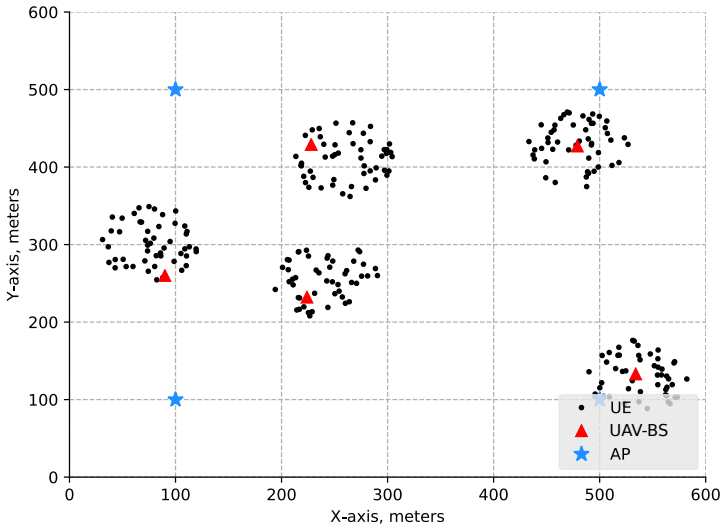

Figure B.4. *PSO-based deployment of 5 UAV-BSs.*